PSEUDO PROJECTION BASED APPROACH TO DISCOVERTIME INTERVAL SEQUENTIAL PATTERN

Dvijesh Bhatt

Department of Information Technology , Institute of Technology, Nirma University Gujarat,(India)

ABSTRACT

Data mining is the process to find out mysteriousand interesting patterns from transactional database. Sequential mining is the one of the major sub-area of data mining to find out the frequent sequences. As straight sequential pattern mining methods do not consider transaction occurrence time intervals, it is impossible to predict the time intervals of any two transactions mined as frequent sequences. There are several constraints to find out the effective and frequent sequential patterns. In this paper, I take time interval between two successive transactions. Time interval sequential mining is the process to find out the frequent sequential patterns with consideration of time interval constraint between two successive truncations. This paper proposed the modify version of the I-Prefixspan algorithm, is called as NI-PrefixSpan, to find out the time interval sequential pattern with pseudo projection table. Later, in this paper identify various advantage and drawback with this approach.

Keywords: Constraints, Data mining, Sequential mining, Time Interval, Time Stamp

I. INTRODUCTION

Data mining [1] is the process of extracting interesting, non-trivial, previously unknown and possibly useful information or patterns from large information sources and data warehouses. For the different types of applications, data and as per user needs, we need different techniques, so many sub-domains of mining was introduced as times goes on. Some of them are Sequential mining, Graph mining, Text mining and information retrieval, Web mining, spatial temporal mining etc.

Sequential mining is process to find out allfrequent sub-sequences from the given sequential dataset [2]. The outcome of this mining process are set of frequent transactions or events,which occurring in an order. Example: ‘A’ event is occurred first and after ‘B’ will occur. In this way sequence patterning is different compare to frequent patterns mining. In frequent patterns mining, order of events does not matter, while in sequential pattern mining order of the events are matter. Sequences always represent in angular brackets. i.e.<a,(ab),c>. Here in this sequence represents three transactions. In first transaction item ‘a’ had been purchased by the customer after that in second transactioncustomer bought both item ‘a’ and ‘b’ in single transaction which is represented by(ab) and in the last transaction customer came to buy item ‘c’. Here, <ab> is totally different sequence than<ba> because here the order of occurrence is mattered. Here, sequence <ab> indicates that item ‘a’ and ‘b’ bought by the customer in two different transactions and sequence <(a,b)> indicates that item ‘a’ and item ‘b’ bought by the customer in single transaction. In this area there are so many algorithms discovered to find out sequence patterns. Algorithms are based on Apriori approach or pattern growth approach. Some of the wildly used Apriori based algorithms are Apriori, GSP [3], SPADE [4], SPAM [5], LAPIN [6], etc. Some of the wildly used pattern growth algorithms are FreeSpan [7] and PrefixSpan [8]. Out of them PrefixSpan is one of

the decent algorithm due to faster calculation and new constraint adopting nature.All these methods do not consider the time interval between any two transactions mined as frequent patterns. In general terms, based on the output patterns, no buddy can judge that how much time will be taken by the customer to do two successive transactions while held 'a' and '(ab)'. To find these kind of frequent sequential pattern, Dr. Chen have introduced the Time Interval Sequential Mining [9] algorithms using both approaches i.e Apriori and pattern growth.. Dr. Chen and his teamshave introduced two algorithms to find out the time interval Sequential mining patterns and those are called as I-Apriori and I-PrefixSpan. So output of this algorithm will be like,having bought a car, a customer will come back to buy a seat cover with in three months and then come back to buy car mobile charger within six months from purchased of seat cover. Here we can see the particular time interval is given between two items, which has been purchased in particular one order. These algorithms are facing sharp boundary problem. To overcome the sharp boundary problem updated version of I-Apriori and I-PrefixSpan had introduced and those algorithms called as FTI-Apriori and FTI-PrefixSpan [10]. In that paper, fuzzy logic was used to overcome sharped boundary problem. Second problem with the I-Apriori and I-PrefixSpan is, these algorithms only show the time interval between two successive events i.e those algorithm never show the how much time will be taken by customer to buy car and car mobile charger. To overcome this restriction, one more version of I-Apriori and I-PrefixSpan was introduced which are called as MI-Apriori and MI-PrefixSpan [11]. Also MLTI-PrefixSpan [12] algorithm was introduced to find out the cross level time interval sequential patterns. Also some on the algorithm also discover integrated sequential patterns mining with fuzzy time interval [13].

II. ANALYSIS OF CURRENT ALGORITHMS

In sequential mining, basically two approach are used to discover frequent sequential patterns i.e Apriori and pattern growth. Both the approaches have some of the advantage and disadvantage with respect to time to generate all sub-sequences, memory is used by algorithm, no of time database scan etc.

First of all let's take a look of advantages and disadvantages of Apriori based approach

Advantage

1. It is really easy algorithm to understand.
2. It is very simple algorithm and find out all frequent sub-sequences from the given sequential data repository.

Disadvantage

1. You have to scan the dataset multiple times to find out frequent sub-sequences, due to this, algorithms takes lots of time to generate the frequent patterns.

   Now let's take a look of advantage and disadvantage of second approach which is pattern growth algorithm which is basically I-PrefixSpan

Advantage

1. It will not scan the main dataset multiple times. Instead of that, algorithm creates projected table for each and every sub-sequences and have to scan projected tables to generate the new frequent sub-sequences.
2. It take comparatively less time to generate all frequent sub-sequences.

   Disadvantage

1. Main drawback of this kind of approach is that you have to generate the projection table for every frequent sub-sequence. For each sub-sequences new projection table are created, due to this you need large amount of main memory to store all the projection tables in it.

   There are many versions of algorithm based on this two approaches to find out the time interval sequential mining. Here in table-1 I list out all them.

III. SOLUTIONS OF THE CURRENT SYSTEM

Here in this section, some of suggestions has been mentioned to overcome the problems of current time interval sequential mining algorithms.

1. So far as per our study, no algorithm has been implemented the pseudo projection table [14] and bi-matrix table which deal with the time interval constraints.
2. PrefixSpan is really good algorithm but still have lack even if we use the pseudo projection. Because even pseudoprojection I-PrefixSpan is stored projected tables in main memory which cost the memory usages and time as well. Also if we have extra-large database then all projection tables are not fit in main memory. To solve problem of PrefixSpan's projection tables one algorithm was proposed to find out frequent sequential patterns and it is called as MEMISP [15], which works as same as the PrefixSpan with pseudoprojection but deal with large database by partition and combine technique.
3. Third solution which is describe, as future enhancement of time interval sequential mining is that use some of the taxonomy or constraints which can eliminate the some of the candidate sequences, which are not frequent, at the beginning of the stage. So it will not waste the time and memory. You can use some of constrains like used in the GSP to make algorithms faster and find only the interesting patterns [16].

Table-1 : List of algorithms for time interval sequential mining

Time Interval Sequential Mining Algorithms			
Sr. No	Name of Algorithms	Year	Descriptions
1	I-Apriori	2003	First algorithm which introduced time interval sequential patterns. It is use typical Apriori base algorithm for that.
2	I-PrefixSpan	2003	First pattern growth algorithm to find the time interval sequential pattern. It is extend version of PrefixSpan.
3	FTI-Apriori	2005	In this algorithm, the boundary of time intervals are not fixed so sharp boundary problem has been resolved. For that fuzzy logic is used. This is Apriori based algorithm.
4	FTI-PrefixSpan	2005	In this algorithm, the boundary of time intervals are not fixed so sharp boundary problem has been resolved. For that fuzzy logic is used. This is pattern growth based algorithm.
5	MI-Apriori	2009	With this algorithm time interval between two non-successive tractions has been calculated. This is Apriori based algorithm.
6	MI-PrefixSpan	2009	With this algorithm time interval between two non-successive tractions has been calculated. This is pattern growth based algorithm.

7	FuzzMI-Apriori	2010	With this algorithm time interval between two non-successive tractions has been calculated. Also the boundary for time interval is not fixed and for that fuzzy logic has been used. This is Apriori based algorithm.
8	FuzzMI-PrefixSpan	2010	With this algorithm time interval between two non-successive tractions has been calculated. Also the boundary for time interval is not fixed and for that fuzzy logic has been used. This is pattern growth based algorithm.
9	MLTI-PrefixSpan	2010	With the help of this algorithm, time interval sequential patterns of cross level can be discovered. For this pattern growth base algorithm PrefixSpan was used.

IV PROPOSED SOLUTION

Now in this paper,we proposed new pseudo projection table approach to generate time interval sequential patterns. As PrefixSpan uses the pseudoprojection to generate the sequential patterns but in this proposed solution the structure of the pseudoprojection table is changes as it uses now generate the time interval sequential patterns. Previously proposed I-PrefixSpan algorithm did not use the pseudo projection table approach so it required much amount of memory to store the data in to main memory. Pseudoprojection table is stored the indexes of the occurrence of the items in the dataset [3]. Pseudo projection table stored (SID, offset). SID indicates specific sequences ID of sub sequences and offset indicates at which place sub-sequence is been in the sequential data repository. In the proposed solution, changes are made the structure of the pseudoprojection table so that we can use the structure to generate the time interval sequential patterns. In proposed structure of the pseudo projection table is contained offset and associate time unit for the specific item in the sequences.In the Table-2is having dataset. In this dataset, every item have time stamp along with it. In the first step, scan the dataset to find out all frequent items.

TABLE-2 DATASET OF TIME INTERVAL SEQUETIAL MINING

Sequence ID	Sequence
10	*<(a,1),(c,3),(a,4),(b,4),(a,6),(e,6),(c,10)>*
20	*<(d,5),(a,7),(b,7),(e,7),(d,9),(e,9),(c,14),(d,14)>*
30	*<(a,8),(b,8),(e,11),(d,13),(b,16),(c,16),(e,20)>*
40	*<(b,15),(f,17),(e,18),(b,22),(c,22)>*

Now consider minimum support is 50%so based on thatitems (a), (b), (c), (d) and (e) are found as frequent items. Item (f) has been eliminated as it do not have the minimum support thresh hold value. Now generate the projection table for all frequent items. Instead of, storing all projection tables in main memory, make the pseudoprojection table. In Table-3 represents modify pseudo projection table. First cell contains 1, 4, 6 that means item ‘a’ is present in sequence ID 10 with 1, 4 and 6 time stamps. Modified pseudo projection table stores the time stamp of the items instead of index of the item. If both items are having same time stamp so it indicates that both items are belongs to same transaction.To generate Time interval sequential pattern, time interval has to be define. Here fix time interval are

$I_0 = 0$; $I_1 = 0 < t \leq 3$ $I_2 = 3 < t \leq 6$ $I_3 = 6 < t \leq$

Number of time intervals and their range are fixed.In this example, three time intervals are there as I_0, I_1, I_2, and $I_3$and their ranges are 0, (0,3] , (3,6] and (6, respecetively. If time interval gap between two successive events is 4 so both items associate with each other with time interval I_2.

TABLE -3 PSEUDOPROJECTION TABLE

SID	<a>	<b>	<c>	<d>	<e>
10	1, 4, 6	4	3,10	∅	6
20	7	7	14	5,9,14	7,9
30	8	8,16	16	13	11,20
40	∅	15,22	22	∅	18

Here [*Sid* : *Pos*] structure has been used**,** where *Sid* is indicating sequence ID and *Pos* is indicating position of item. Based on this, five postfix sequences in the projected database is generated. In proposed solution, this kind of projection table would not store in main memory. This is just for the easy understanding.

[10:1] ((*c*, 3)(*a*, 4)(*b*, 4)(*a*, 6)(*e*, 6)(*c*, 10)),

[10:4] ((*b*, 4)(*a*, 6)(*e*, 6)(*c*, 10)),

[10:6] ((*e*, 6)(*c*, 10)),

[20:7] ((*b*, 7)(*e*, 7) (*d*, 9)(*e*, 9)(*c*, 14)(*d*, 14)),

[30:8] ((*b*, 8)(*e*, 11)(*d*, 13)(*b*, 16)(*c*, 16), (*c*, 20)).

Now generation of the frequent sequential pattern, time interval table has been generated, which looks like table-4.In the table, 1st column indicated the time interval and 1st raw will indicate the frequent items. Remaining cells indicate the frequency of data occurrence with particular time interval. Using this data, 2-length sub-sequences is generated. Time interval gap can be calculated by the simple subtraction of the time stamp associate with respective items. If time interval between both items is zero, so it indicates that both the items have been purchased in the single transaction. From table-3, we can calculate time interval between two itemswhich is useful to generate table-4. Here in sequence ID 10, item ‘a’ is occurred with time stamp 1, 4 and 6 and ‘b’ occurred at time 4 as well. Now considering time stamp of item ‘a’ as 1 and time stamp of item‘b’ as 4, so time interval between them is: | 1– 4 | = 3 which belongs to I_1. So, now just increase the counter of cell B-I_1 by one. Based on this time interval table is created. Observing from the table-4, cellB-I_0 is frequent because it is stratifying minimum support criteria. Now from table-4, length-2 time interval sequential patter has been generated. Thus, (a, I_0, b) is the frequent sequence. That means customer bought item ‘a’ and item ‘b’ in single transactionmore frequently.

TABLE-4The table constructed in NI-PrefixSpan((*a*), 1, *S* | (*a*))

Table	A	B	C	D	E
I_0	0	3	0	0	2
I_1	1	1	1	1	3
I_2	1	0	1	1	1
I_3	0	1	3	1	0

So here (a, I_0, b), (a, I_0, e), (a, I_1, e) and (a, I_3, c) are the frequent sub-sequences. Now we also have to make the index of these frequent items. Suppose we take (a, I_0, b) as one sequence so we have to make the index for it.

And it will be 4, 7, 8 respectively for the sequence ID 10, 20 and 30. Now repeat this step until discovering of all frequent sub-sequence. Suppose now we take (a, I_0, b) and make projection table of this. So we will get

[10:4]: ((*a*, 6)(*e*, 6)(*c*, 10))

[20:7]: ((*e*, 7)(*d*, 9)(*e*, 9)(*c*, 14)(*d*, 14))

[30:8]: ((*e*, 11)(*d*, 13)(*b*, 16)(*c*, 16)(*c*, 20))

Base on that we make another table same like Table-4.

Table-5 NI-PrefixSpan(((a, I_0, b), 4, S | (a, I_0, b)))

Table	B	C	E
I_0	0	0	1
I_1	0	0	3
I_2	0	1	0
I_3	1	2	0

Now, from the Table-5 that cell (I_1, e) and (I_3, c) is satisfying minimum support thresh hold. Base on that find 3-length sub-sequences are (a, I_0, b, I_1, e) and (a, I_0, b, I_3, c).And again have to make the pseudoprojection table or index for the new sub-sequences.

Advantage of pseudoprojection table is that projection table is not stored in main memory. Thus, it is utilizationof main memory. Also, do not need to scan main database multiple times and there is no need to generate the projection table for each and every sub-sequences. But one disadvantage of this method is stored whole dataset into main memory. One possible solution for the this problem is, store some patterns in pseudo projection table and some patterns in physical projection. Combination of both projection techniques can solve the current shortcoming of NI-PrefixSpan. When data shrink enough to store in main memory all dataset will be move to the main memory otherwise both memory can be used to store the dataset.

IV. CONCLUSION

In this paper, Iproposed new algorithm NI-PreifixSpan to discover time interval sequential patternswith the help of modify pseudo projection table which stores the time stamp value of different items instead of its index in sequence ID. Also algorithm solved two major problem which are related to memory and no of time main dataset will be scannedwill be reduced. In future extension of the NI-PrefixSpan can be in two way, one is to improve the performance of the current algorithm and second apply same algorithm to find multiple time interval sequential patterns.

REFERENCES

[1] J. Han and M.Kamber, “Data Mining – Concepts & Techniques”, Morgan Kaufmann Publishers (Academic Press), 2001.

[2] R. Agrawal and R. Srikant, “Mining sequential patterns”, International Conference of Data Engineering (ICDE
’95), 1995.

[3] R. Srikant and R. Agrawal, “Mining sequential patterns: Generalizations and performance improvements”, Proceedings of the 5th International Conference Extending Database Technology, 1057, pp. 3-17, 1996.

[4] M. Zaki, “SPADE: An efficient algorithm for mining frequent sequences”, Machine Learning, vol.40 pp. 31-60 2001.

[5] J.Ayres, J. Flannick, J. Gehrke, and T. Yiu, “Sequential pattern mining using a bitmap representation”, Proc.OfInternational Conference on Knowledge Discovery and Data Mining, 2002.

[6] Zhenglu Yang; Kitsuregawa, M., "LAPIN-SPAM: An Improved Algorithm for Mining Sequential Pattern," *Data Engineering Workshops, 2005. 21st International Conference on* , vol., no., pp.1222,1222, 05-08 April 2005

[7] J. Pei, J. Han, B. Mortazavi-Asi and H. Pino, “PrefixSpan: Mining Sequential Patterns Efficiently by Prefix-Projected Pattern Growth”, International Conference of Data Engineering(ICDE'01), 2001.

[8] J. Han, G. Dong, B. Mortazavi-Asl, Q. Chen, U. Dayal and M.-C. Hsu,“FreeSpan: Frequent pattern-projected
sequential pattern mining”, Proc. 2000 International Conference of Knowledge Discovery and Data Mining (KDD’00), pp. 355-359, 2000.

[9] Chen, Y.L., Chiang, M.C. and Ko, M.T. (2003). "Discovering time- interval sequential patterns in sequence databases," Expert Syst. Appl., Vol. 25, No. 3, (pp. 343-354).

[10] Chung-I Chang; Hao-En Chueh; Lin, N.P., "Sequential Patterns Mining with Fuzzy Time-Intervals," *Fuzzy Systems and Knowledge Discovery, 2009. FSKD '09. Sixth International Conference on* , vol.3, no., pp.165,169, 14-16 Aug. 2009

[11] Ya-Han Hu, Tony C. Huang, Hui-Ru Yang, Yen-Liang Chen, “On mining multi-time-interval sequential patterns”, Data & Knowledge Engineering, Vol. 68, No. 10. pp. 1112-1127,(23 Oct 2009).

[12] Ya-Han Hu; Fan Wu; Chieh-I Yang; , "Mining multi-level time-interval sequential patterns in sequence databases," Software Engineering and Data Mining (SEDM), 2010 2nd International Conference on , vol., no., pp.416-421, 23-25 June 2010.

[13] Chung-I Chang; Hao-En Chueh; Yu-Chun Luo, "An integrated sequential patterns mining with fuzzy time-intervals," *Systems and Informatics (ICSAI), 2012 International Conference on* , vol., no., pp.2294,2298, 19-20 May 2012.

[14] Dvijesh Bhatt and Kiran amin;, “A-Survey Time Interval Sequential Mining”, International Conference on recent trend in computer science and engineering (ICRTCSE 2012), May-2012.

[15] M.Y. Lin and S.Y. Lee, "Fast Discovery of Sequential Patterns through Memory Indexing and Database Partitioning," *J. Information Science and Eng.*, vol. 21, pp. 109-128, 2005.

[16] J. Pei, J. Han and W. Wang, “Constraint-based sequential pattern mining: the pattern growth methods”, J Intell.Inf. Syst, Vol. 28, No.2, pp. 133 –160, 2007.

ENHANCING WEAR RESISTANCE OF GREY CAST IRON USING AL_2O_3-3TiO_2 AND AL_2O_3-13TiO_2 COATINGS

Gobind[1], Dr. Neel Kanth Grover[2] & Jawala Parshad[3]

[1]*Department of Mechanical Engineering, S.B.S.S.T.C, (Polywing), Ferozepur (India)*

[2,3]*Department of Mechanical Engineering, S.B.S.S.T.C, Ferozepur (India)*

ABSTRACT

Failure of mechanical components due to wear is the most common and unavoidable problem in automobiles, power generation units (hydro power plants), construction equipments, marine sector, gas and fuel pipelines and other mechanical processing industries. It not only affects the life of a component but also reduces its performances. Therefore due to heavy economic losses associated with wear, this problem has attracted the attention of the researchers worldwide. To overcome this problem of wear, wear resistant alloys or suitable wear resistant coatings deposited by various advanced techniques are generally used. Now a day's Detonation gun spray coatings are gaining popularity due to exceptional hardness, wear resistance and cost effectiveness. In wire drawing pulleys the friction between the Pulley and wire leads to the wear of pulley. In this study Al_2O_3-3TiO_2 and Al_2O_3-13TiO_2 coatings were prepared on grade of cast iron (grey iron grade 250). The samples are investigated through standard procedure of pin-on-disk tests. The rotating disc at 1m/s is subjected to pressures of 30, 40, 50N. The samples were weighed before and after the test. And the results of coated samples were compared with the uncoated samples.

Keywords: Wear, Grey Cast Iron, Coating, Detonation Gun, Test.

I.INTRODUCTION

Surface engineering is the sub-discipline of materials science which deals with the surface of solid matter. Solids are composed of a bulk material covered by a surface. The surface which bounds the bulk material is called the Surface phase. It acts as an interface to the surrounding environment. The bulk material in a solid is called the Bulk phase. The surface phase of a solid interacts with the surrounding environment. This interaction can degrade the surface phase over time. Environmental degradation of the surface phase over time can be caused by wear, corrosion, fatigue and creep [1].Surface engineering can be defined as the branch of science that deals with methods for achieving the desired surface requirements and their behavior in service for engineering components [2].

1.1 Wear

In materials science, wear is considered to be the erosion of material from a solid surface by the action of another solid. According to the German DIN standard 50 320, "*the progressive loss of material from the surfaces of contacting body as a result of mechanical causes*" is defined as wear. The parameters that affect

wear are loads, speed, temperature, contact type, type of environment etc. The wear is the loss of material and is expressed in terms of volume. Wear is a process of removal of material from one or both of two solid surfaces in solid state contact, occurring when two solid surfaces are in sliding or rolling motion together according to Bhushan and Gupta (1991). The rate of removal is generally slow, but steady and continuous.

The prediction and control of wear is one of the most essential problems emerging in the design of cutting operations. A useful definition for a worn out part is: "*A part is considered to be worn out when the replacement cost is less than the cost for not replacing the part*" [3]. Part failure is said to occur when it no longer performs the desired function whereas total failure (ultimate failure) is defined as the complete removal of the cutting edge, a condition obtaining when catastrophic failure occurs. The wear problem selected as case study in this thesis work is being faced in wire drawing pulleys, brake disc rotors. Wear is the gradual removal of material obtained at contacting surfaces in relative motion. While friction results in important energy losses, wear is associated with increased maintenance costs and costly machine downtime. Wear is caused due to many factors but friction is most important of them. Few more causes for occurrence of wear can be: Improper component design, Excessive Pressure, Contact area, Inadequate Lubrication, Environment, Material properties. Wear includes six principal, quite distinct phenomena that have only one thing in common: the removal of solid material from rubbing surfaces. These are (1) adhesive; (2) abrasive; (3) fatigue; (4) impact by erosion or percussion; (5) corrosive; and (6) electrical arc-induced wear. The wear resistance in the case of brake disc rotors, wire drawing pulleys etc. can be improved by a wide range of coatings. . The principle of thermal spray is to melt material feedstock (wire or powder), to accelerate the melt to impact on a substrate where rapid solidification and deposit build-up occurs. To reduce the wear problem, wear resistant coatings are deposited on the grey cast irons. Standard test methods for wear testing with pin-on disc apparatus are employed to study the wear behavior of the uncoated and coated grey irons as well. Thermal spray processes that have been considered to deposit the coatings are enlisted as: (1) Flame spraying with a powder or wire, (2) Electric arc wire spraying, (3) Plasma spraying, (4) Spray and fuse, (5) High Velocity Oxyfuel (HVOF) spraying, (6) Detonation Gun. Among the commercially available thermal spray coating techniques, detonation spray (DS) is chosen to get hard, dense and consequently wear resistant coatings

1.2. Detonation Gun Spraying Process

In detonation Gun spraying Process, as shown in (figure 1), a mixture of spray material, acetylene and oxygen is injected into the detonation chamber. A precisely measured quantity of the combustion mixture consisting of oxygen and acetylene is fed through a tubular barrel closed at one end. In order to prevent the possible back firing a blanket of nitrogen gas is allowed to cover the gas inlets. Simultaneously, a predetermined quantity of the coating powder is fed into the combustion chamber. The gas mixture inside the chamber is ignited by a simple spark plug. The combustion of the gas mixture generates high pressure shock waves detonation wave), which then propagate through the gas stream. Depending upon the ratio of the combustion gases, the temperature of the hot gas stream can go up to 4000 deg C and the velocity of the shock wave can reach 3500m/sec. The hot gases generated in the detonation chamber travel down the barrel at a high velocity and in the process heat the particles to a plasticizing stage (only skin melting of particle) and also accelerate the particles to a velocity of 1200m/sec. These particles then come out of the barrel and impact the component held by the manipulator to form a coating. The high kinetic energy of the hot powder particles on impact with the substrate result in a buildup of a very dense and strong coating. The coating thickness developed on the work piece per shot depends on the ratio of

combustion gases, powder particle, size carrier gas flow rate, frequency and distance between the barrel end and the substrate Depending on the required coating thickness and the type of coating material the detonation spraying cycle can be repeated at the rate of 1-10 shots per second [4]. The chamber is finally flushed with nitrogen again to remove all the remaining "hot" powder particles from the chamber as these can otherwise detonate the explosive mixture in an irregular fashion and render the whole process uncontrollable. With this, one detonation cycle is completed above procedure is repeated at a particular frequency until the required thickness of coating is deposited.

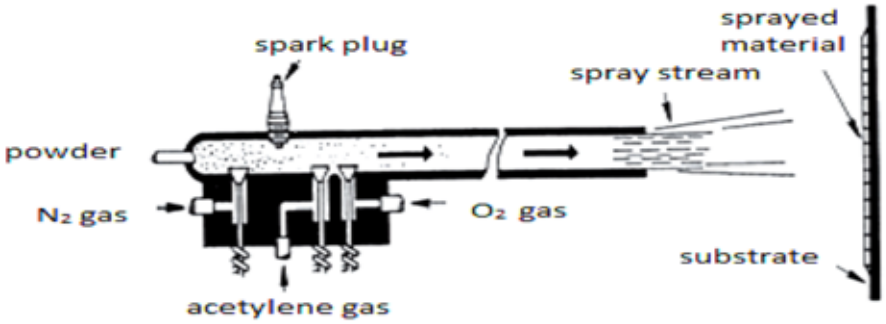

Figure.1 Detonation Gun process

The chamber is finally flushed with nitrogen again to remove all the remaining "hot" powder particles from the chamber as these can otherwise detonate the explosive mixture in an irregular fashion and render the whole process uncontrollable. With this, one detonation cycle is completed above procedure is repeated at a particular frequency until the required thickness of coating is deposited [5].

II. EXPERIMENTAL PROCEDURE

Samples of cylindrical shape, with diameter 8mm and length 30mm were casted with the component of GI250. The grinding of end faces (to be coated) of the pins is done using emery papers and grinding was followed by polishing with 1/0, 2/0, 3/0 and 4/0 grades polishing papers. Two types of coating powders namely 1) Al_2O_3-$3TiO_2$ 2) Al_2O_3-$13TiO_2$ are selected for Detonation Spray Coating Process after the literature survey. Powder Al_2O_3-$3TiO_2$ and Al_2O_3-$13TiO_2$ form hard dense and excellent bonded coatings on the samples. The wear tests were performed in a machine (Wear and Friction Monitor Tester TR-201) conforming to ASTM G 99 standard. The wear tests for coated as well as uncoated specimens were conducted under three normal loads of 30 N, 40 N and 50 N and a fixed sliding velocity of 1 m/s. A track diameter of D=40 mm, sliding speed v=1 m/s is kept. Wear tests have been carried out for a total sliding distance of 5400 m (6 cycles of 5min, 5min, 10min, 10min, 20min, 40min duration). Weight losses for pins were measured after each cycle to determine the wear loss. The coefficient of friction has been determined from the friction force and the normal loads in all the cases. The results of coating volume loss are reported.

II.RESULTS AND DISCUSSION

Comparative Wear Behavior for two coatings

The comparison of wear loss for the coatings; Al_2O_3-3TiO_2 and Al_2O_3-13TiO_2 on GI250 at 30N, 40N, and 50N is as shown in Figure 2. From the bar chart it is clear that Al_2O_3-13TiO_2 shows minimum CVL as compared to Al2O3-3TiO_2 coating. CVL for Al_2O_3-13TiO_2 is least at all the three normal loads of 30N, 40N, 50N, whereas highest CVL is found to be in bare GI250 substrate. CVL for both the detonation sprayed coatings is less than that to found in the in bare GI250. The CVL for all the three substrate in increasing order can be given as Bare GI250 > Al_2O_3-3TiO_2 > Al_2O_3-13TiO_2 Which means that Al2O3-13TiO2 coated substrate is most wear resistant among the three substrates and bare GI250 substrate is least wear resistant. The difference in CVL of Al_2O_3-3TiO_2 and Al2O3-13TiO2 coatings is not much but still Al_2O_3-13TiO_2 proves to be better wear resistant among the two at all three loads.

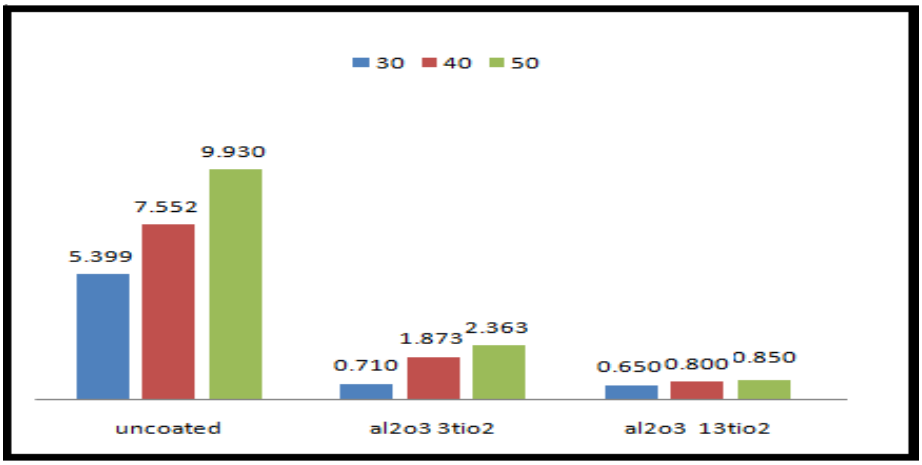

Figure 2: Cumulative Volume loss (mm3) in one cycle for D-gun sprayed coatings and bare GI250 At 30N, 40N and 50N

IV.CONCLUSION

Based upon experimental results obtained in the present work, the following conclusions have been drawn:

- Detonation Sprayed Al_2O_3-3TiO_2, Al_2O_3-13TiO_2 coatings have successfully been deposited on GI250 grade of grey cast iron.
- The detonation sprayed Al_2O_3-3TiO_2 & Al_2O_3-13TiO_2 coated GI250 specimens showed significantly lower cumulative volume loss as compared to bare GI250 material.
- Cumulative Volume loss for detonation sprayed Al_2O_3-3TiO_2 & Al_2O_3-13TiO_2 coated as well as bare GI250 specimens increases with increase in load.
- The Cumulative Volume loss for Al_2O_3-13TiO_2 coating was observed to be minimum in the present study.
- The Al_2O_3-13TiO_2 coating substrate combination has shown minimum Cumulative Volume loss among all the combinations. The wear resistance for coating–substrate combination in their Increasing order (at 50N) is Al_2O_3-13TiO_2 > Al_2O_3-3TiO_2 > Bare GI250

REFERENCES

[1] R.Chattopadhyay, 'Advanced Thermally Assisted Surface Engineering Processes' Kluwer Academic Publishers, MA, USA (now Springer, NY), 2004, ISBN 1-4020-7696-7, E-ISBN1- 4020-7764-5.

[2] Halling, J., (1985), "Introduction: Recent Development in Surface Coating and Modification Processes", MEP, London.

[3] N. P. Petrov, Inzh. Zfc. St-Peterb. 4 (1883) 535–564.

[4] Goyal Rakesh, Sidhu Buta Singh, Grewal J.S.; "Surface Engineering and Detonation Gun Spray Coating", International Journal of Engineering Studies, Volume 2, Number 3 (2010), 351-357.

[5] Lakhwinder Singh, Vikas Chawla, J.S. Grewal (2012) "Journal of Minerals & Materials Characterization & Engineering" Vol. 11, No.3, pp.243-265.

IMPROVING WEAR BEHAVIOR OF GREY CAST IRON BY WC–12CO AND STELLITE-6 COATINGS

Gobind[1], Ankush Batta[2] & Rajnesh Kumar[3]

[1,2,3]*Department of Mechanical Engineering, S.B.S.S.T.C, Ferozepur, Punjab,(India)*

ABSTRACT

The wear is very severe problem in industry. It leads economic loss to society. In the present research study efforts will be made to reduce the wear rate of Braking Disc Rotor with surface modifications techniques and comparison of wear properties grade of cast iron GI250 coated by WC–12CO and Stellite-6 deposited by Detonation spray processes is presented. These samples are investigated through standard procedure of pin-on-disk tests. The rotating disc at 1m/s is subjected to pressures of 40N, 50N and 60N.. The samples were weighed before and after the test. And the results of coated samples were compared with the uncoated samples. The results show that the WC-12CO on GI250 grey cast iron performs slightly better than the Stellite-6 coating. The WC-12CO- GI250 coating substrate combination has shown minimum Cumulative Volume loss among all the two combinations. The wear resistance for coating–substrate combinations in their decreasing order is WC-12CO-GI250>Stellite6-GI250.

Keywords: Wear, Detonation Spray, Brake Disc Wear Resistance

I. INTRODUCTION

Surface engineering deals with the surface design and performance of solid materials. The life of a component depends on the surface characteristics of engineering materials. Surface engineering can be defined as the branch of science that deals with methods for achieving the desired surface requirements and their behavior in service for engineering components [1].

1.1 Wear

Wear is the removal of material from one or both of two solid surfaces in a solid-state contact. It occurs when solid surfaces are in a sliding, rolling, or impact motion relative to one another. Wear occurs through surface interactions at asperities, and components may need replacement after a relatively small amount of material has been removed or if the surface is unduly roughened. In well-designed tribological systems, the removal of material is usually a very slow process but it is very steady and continuous [2]. Wear is caused due to many factors but friction is most important of them. Few more causes for occurrence of wear can be: Improper component design, Excessive Pressure, Contact area, Inadequate Lubrication, Environment, Material properties. Wear includes six principal, quite distinct phenomena that have only one thing in common: the removal of solid material from rubbing surfaces. These are (1) adhesive; (2) abrasive; (3) fatigue; (4) impact by erosion or percussion; (5) corrosive; and (6) electrical arc-induced wear [3].

Thermal spray is a technique that produces a wide range of coatings for diverse applications. The principle of thermal spray is to melt material feedstock (wire or powder), to accelerate the melt to impact on a substrate where rapid solidification and deposit build-up occurs [4]. To reduce the wear problem, wear resistant coatings are deposited on the grey cast irons. Standard test methods for wear testing with pin-on disc apparatus are employed to study the wear behavior of the uncoated and coated grey irons as well. Thermal spray processes that have been considered to deposit the coatings are enlisted as: (1) Flame spraying with a powder or wire, (2) Electric arc wire spraying, (3) Plasma spraying, (4) Spray and fuse, (5) High Velocity Oxyfuel (HVOF) spraying, (6) Detonation Gun.

D-gun spray process is a thermal spray coating process, which gives an extremely good adhesive strength, low porosity and coating surface with compressive residual stresses [5].

Therefore Among the commercially available thermal spray coating techniques, detonation spray (DS) is chosen to get hard, dense and consequently wear resistant coatings.

1.2. Wear rate

The wear rate data for the coated as well as uncoated specimens were plotted with respect to sliding distance to establish the wear kinetics. The specific wear rates for the coated and uncoated material were obtained by $W = \delta w / L\rho F$ Where W denotes specific wear rates in, Bowden (B) (1B=10-6 mm3/N-m) [Recommendation from IRG OECD meeting with about 30 participants to introduce a new unit for wear rate: Bowden (B) equal to 10-6 mm3/N.m] δw is the weight loss measured in, g L the sliding distance in, m ρ the density of the worn material in g/ mm3 and F the applied load in N.

1.3. Wear volume

The wear volume loss was also calculated from the weight loss and density of the coatings as well as substrate material for all the investigated cases. These data were reported in the form of plots showing the cumulative wear volume loss Vs sliding distance for all the cases. Bar charts were also drawn to show net Volume = mass / density Wear Volume Loss = $(\delta w/9.81) /\rho$ Where δw is the weight loss in, g And ρ is the density of material, g/mm3.

1.4. Coefficient of friction

The coefficient of friction (μ) determined from the frictional force and the normal load has been plotted against the sliding time to give the friction behavior of the coated as well as the uncoated material. The coefficient of friction (μ) was calculated as below: μ = Frictional Force (N) / Applied Normal Load (N)

II.EXPERIMENTAL PROCEDURE

Samples of cylindrical shape, with diameter 8mm and length 30mm were casted with the component of GI250 substrate. The grinding of end faces (to be coated) of the pins is done using emery papers and grinding was followed by polishing with 1/0, 2/0, 3/0 and 4/0 grades polishing papers. Two types of coating powders namely and (1) WC–12CO (2) Stellite-6 are selected for Detonation Spray Coating Process after the literature survey. Powder WC–12CO & Stellite-6 form hard dense and excellent bonded coatings on the samples. The wear tests

were performed in a machine (Wear and Friction Monitor Tester TR-201) conforming to ASTM G 99 standard. The wear tests for coated as well as uncoated specimens were conducted under three normal loads of 40N, 50N and 60N**.** And a fixed sliding velocity of 1 m/s. A track diameter of D=40 mm, Sliding speed *v*=1 m/s is kept. Wear tests have been carried out for a total sliding distance of 5400 m (6 cycles of 5min, 5min, 10min, 10min, 20min, 40min duration). Weight losses for pins were measured after each cycle to determine the wear loss.
The coefficient of friction has been determined from the friction force and the normal loads in all the cases. The results of coating volume loss are reported.

III.RESULTS AND DISCUSSION

3.1.1 Characterization of Coatings

3.1.1.1 SEM/EDS analysis of the D-gun as sprayed coatings

The Scanning electron microscope micrographs as well as Energy Dispersive Spectrum (EDS) with element composition for Detonation sprayed Stellite-6 and WC-12CO coatings on GI250 shown in **Figure (3.1).** The microstructure of these coatings is hardly bonded, homogeneous and free from surface cracks, pores and voids. The SEM/EDS analysis of the stellite-6 coating showed in Figure (3.1(a)).The elements for stellite-6 coating corresponding to (spectrum 1) for load 40N and 50N are C, O, Cr, CO Si etc. The color of the surface at this spectrum is dull grey and near this point surface is white which may be due to presence of oxygen and at (spectrum 4) the coating is more uniform. The elemental composition for WC-12CO coating corresponding to spectrum 1 & 4 for load 40N and 50N is shown in (Figure 3.1(b)). The spectrum 4 of WC-12CO coating also confirms the presence of desired coating elements Chromium (32.72%), Cobalt (46.58%) and Tungsten (20.70%). At (spectrum 4) the color is naturally white which is may be due presence of excess oxygen on the surface.

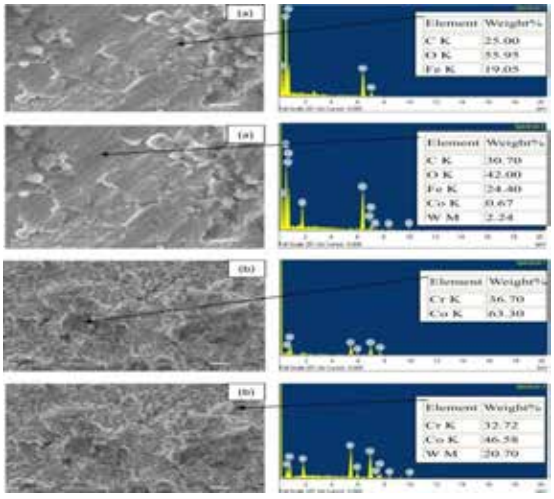

Figure 3.1 Surface Morphology and EDS patterns from different spots on as coated samples (a) Stellite-6

(b) WC-12CO.

3.1.1.2 X-Ray Diffraction (XRD) Analysis

The X-ray diffraction patterns for detonation sprayed stellite-6 and WC-12CO ON GI250 are shown in **Figure 3.2**. Figure 3.2 (a) shows the X-ray diffraction patterns for as coated samples of Stellite-6 coating on GI250 and Figure 3.2(b) shows the X-ray diffraction patterns for as coated samples of WC-12CO coating on GI250. From Figure 3.2 (a) it is identified that coating stellite-6 shows the excess of desired coating elements such as C, Cr, O, Co and small amount of Fe and Si. Similarly, from Figure 3.2(b) it is evident that coating WC-12CO shows the major phases of tungsten which is desired element of coating and minor phases of C and O which together to make Co which is also desired element of coating WC-12CO. The no. of peaks corresponding to elements of coatings can be seen from diffraction patterns of different coatings for GI250.

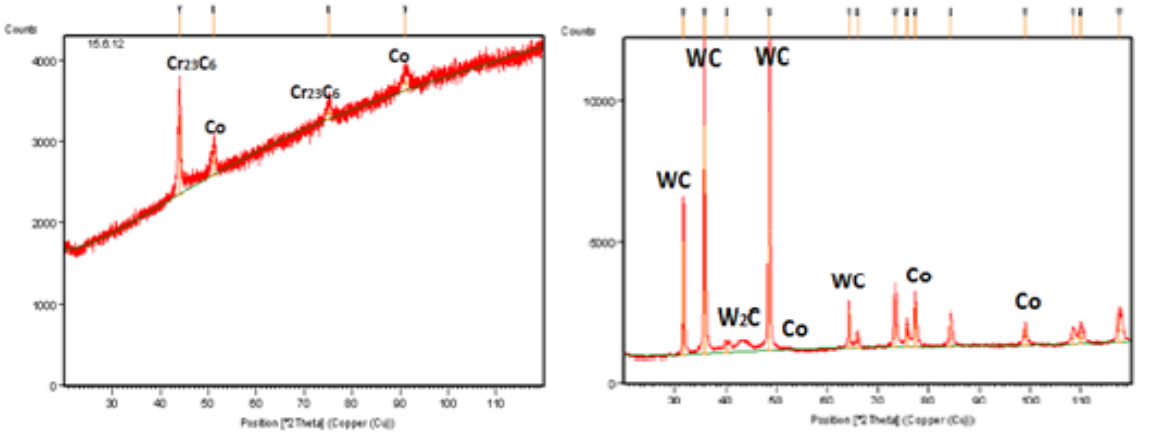

Figure 3.2 X-ray Diffraction patterns of as coated GI250 material; (a) Stellite-6 (b) WC-12CO

3.1.2 Wear Behavior

3.1.2.1. Substrate GI250 3.1.2.1.1.

Wear Behavior of Two coatings vs GI250 Three samples of each coating i.e. Stellite-6 and WC-12CO on GI250 were subjected to wear on Pin-On–Disc-wear test rig at normal loads of 40N, 50N and 60N respectively. Three samples of bare GI250 substrate were also subjected to wear on Pin-On Disc-wear test rig at the same loads. The cumulative volume loss vs time for each coating is plotted as shown in **Figure 3.4.** From the results of (Figure 3.4) it is investigated that cumulative volume loss for two detonation sprayed wear resistant coatings show better wear resistant in comparison to bare GI250. The bar chart (**Figure 3.5**) showing the Cumulative Volume Loss (CVL) in one complete cycle (90 min) is also drawn for each coating and bare GI250 substrate. From (**Figure 3.4 & Figure 3.5**) it is observed that with increase in load wear loss increases for the detonation sprayed coatings Stellite-6 and WC-12CO and bare GI250 the observation is same as that of the observation of (Cueva, 2003).

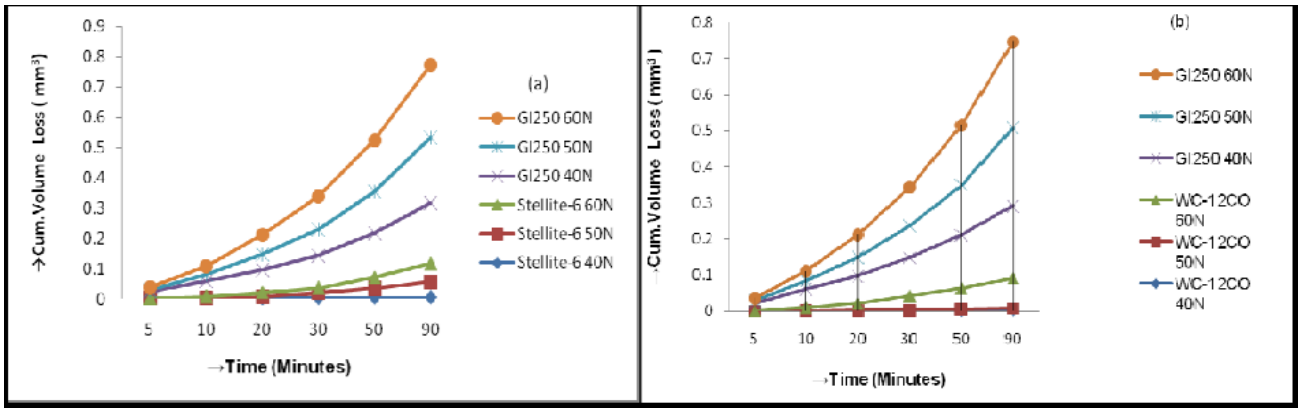

Figure 3.4 Cumulative Volume Loss (Mm3) With Time For (A) Stellite-6 (B) WC-12CO Coatings and GI250 substrate.

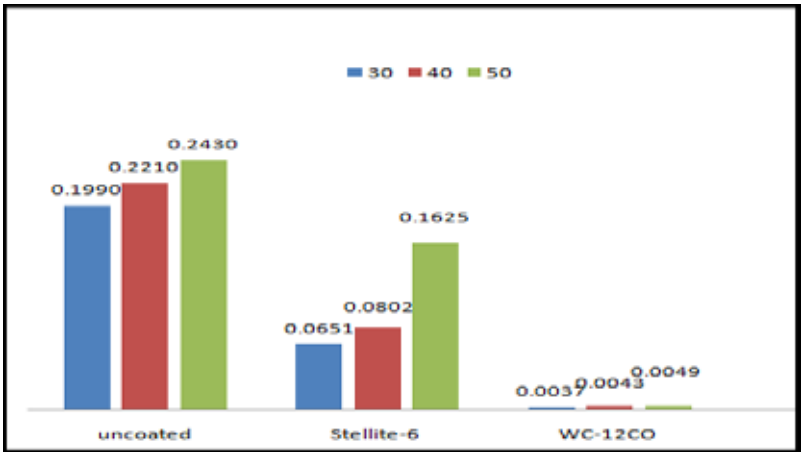

Figure 3.5 Cumulative Volume loss (mm3) in one cycle for D-gun sprayed coatings and bare GI250 at 40N, 50N and 60N.

3.1.2.1.2 Comparative Wear Behaviour for two coatings

Figure 3.6 shows Comparative Volumetric Wear Loss (mm3) for two coatings at (a) 40 N (b) 50 N and (c) 60 N. It is also observed from the results that WC-12CO is showing the minimum cumulative volume loss as compared to other two coatings. Therefore the wear resistance of Detonation sprayed coatings on GI250 in their decreasing order can be given as WC-12CO>Stellite-6.

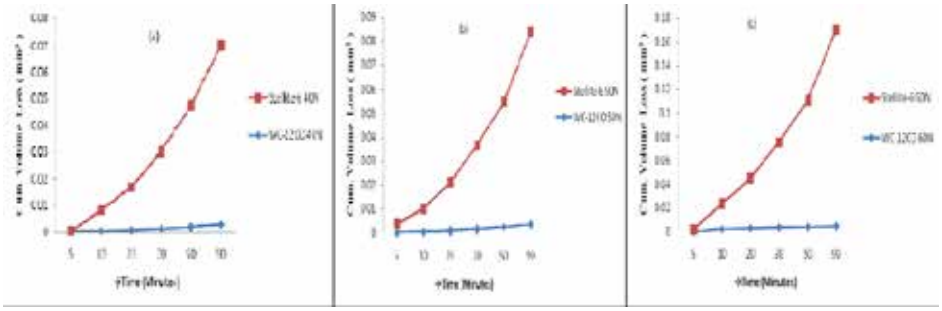

Figure 3.6 Comparative Volumetric Wear Loss (Mm3) For Two Coatings On GI250 Substrate At (A) 40 N (B) 50 N And (C) 60.

IV DISCUSSION

Selection of material, coating and the wear behavior of the uncoated GI250 and detonation sprayed Stellite-6 and WC-12CO coatings have been discussed. From the study of Mohanty, 1996 it was observed that it is possible to deposit almost any material on any substrate by D-gun spray process to considerably extend the life of parts; also it is observed in the present study that the Stellite-6 and WC-12CO coatings powders have been successfully deposited on GI250 substrate by the detonation spray process. It was further confirmed by characterization of coatings using SEM and EDAX analysis of as coated specimens. SEM/EDAX results of WC-12CO and Stellite-6 (Figure 3.1 (a & b)) shows the presence of O and C on the surface which may be due to formation of carbide. Also XRD analysis of study did (Figure 3.2) which supports the results of scanning electron microscope (SEM). There is always the material loss of bare material greater than the as coated material. From (Figure 3.4) it is observed that the detonation sprayed wear resistant coatings Stellite-6, WC-12CO coated GI250 specimens showed significantly lower cumulative volume loss as compared to bare GI250 material under the normal load of 40N, 50N and 60N. It is investigated with the help of Pin-on-Disk Wear testing machine. There are many studies; Murthy & Venkataraman, 2006, Sundararajan, 2005 and Jun Wang 2000 which support the above finding that Detonation sprayed coatings increases the wear resistant and wear loss of bare material is always greater than the as coated material which is also found in present study in (Figure 3.4).Also Figure 3.6 shows comparison of two coatings in which WC-12CO has minimum wear loss as compared to Stellite-6 and therefore WC-12CO can be used for coating the grey cast iron material which is used in light truck pads. WC-12CO coating has more bonding strength than stellite-6. From (Figure 3.6) it is observed that the wear loss is increase with increase load. From this figure it is clear that the wear loss for two coatings and bare GI250 also increases with load which is same observation as Cueva (2003), The CVL for WC-12CO coating was found to be minimum in present study as shown in Figure 3.5 and Figure 3.8.it is may be due to the presence of W, CO, FE and O also tungsten and carbide increases the property of wear resistant. Identical results have been reported by Mohanty, 1996. It may be due to carbide formation due to diffusion of the Fe from the substrate. The WC-12CO-GI250 coating substrate combination has shown minimum wear loss among all four combinations as shown in Figure 3.6.

V.CONCLUSIONS

Based upon experimental results obtained in the present study, the following conclusions have been drawn:

1. GI250 is best grade of grey cast iron.
2. Stellite-6 and WC-12CO are best coating powders to deposit on grey cast irons (GI250).
3. Stellite-6 and WC-12CO wear resistant coatings have successfully been deposited on GI250 Grade of grey cast iron.
4. The Stellite-6 and WC-12CO coating based GI250 specimens showed lower cumulative Volume loss as compared to bare GI250 specimens.
5. Wear loss for detonation sprayed wear resistant coatings Stellite-6 and WC-12CO coated Samples and bare GI250 samples increases with increase in load.
6. The Cumulative Volume loss for WC-12CO coating was minimum in the present study.Therefore WC-12CO is best coating to deposit on GI250 grade of grey cast irons.

7. The wear resistance for coating–substrate combinations in their decreasing order is WC-12CO-GI250 > Stellite-6- GI250. Therefore out of these combinations WC-12CO-GI250 Coating substrate combination is the best Combination.

REFERENCES

[1] Halling, J., (1985), "Introduction: Recent Development in Surface Coating and Modification Processes", MEP, London.

[2] Archard, J. F. 1980. Wear theory and mechanisms. Wear Contro Handbook, ed. M. B. Peterson and W. O. Winer, pp. 35-80.ASME, New York

[3] Manoj Kumar Singla, Harpreet Singh , Vikas Chawla,"Thermal Sprayed CNT Reinforced Nanocomposite Coatings" Vol. 10, No.8, pp.717-726, 2011.

[4] S.K. Basu, S.N. Sengupta and B.B. Ahuja, Fundamentals of Tribology (Prentice-Hall of India Pvt. Ltd., New Delhi, 2005).

[5] Rajasekaran B., Sundara Raman Ganesh S., Joshi S.V., Sundararajan G.; "Influence of detonation gun sprayed alumina coating on AA 6063 samples under cyclic loading with and without fretting", Tribology International, Volume 41, (2008), 315–322.

LUNG SEGMENTATION IN DIGITAL CHEST X-RAY IMAGES USING GRAPH CUT OPTIMIZATION METHOD

Mrs. N. Ravia Shabnam Parveen

Assistant Prof (SG), Department of MCA,

Final Year M.E (CSE), KLN College of Engineering, Madurai (India)

ABSTRACT

Chest X-Ray are Gray scale images used to diagnose or monitor treatment for conditions of pneumonia, emphysema, lung cancer, line and tube placement and tuberculosis by Physicians. This work is an attempt to extract the Lung Boundary so that it can trace severity of any infection and it is divided into three segments. 1. Content-based image retrieval approach for identifying training images (with masks) most similar to the patient CXR using a partial Radon transform and Bhattacharyya shape similarity measure. 2. Creating the initial patient-specific anatomical model of lung shape using SIFT-flow for deformable registration. 3. Extracting refined lung boundaries using a graph cuts optimization approach with a customized energy function. In earlier approach the accuracy rate was 95.4%. By combining the Integral values, this work tries to increase the accuracy level by 97.5%. This is done by optimizing the graph cut values. This research work will help the Doctors to identify the severity of the infection with the chest X-Ray image itself, instead of going for other expensive diagnosis tests.

Keywords: Chest X-Ray Imaging, Computer-Aided Detection,Image Registration, Image Segmentation, Pneumonia Infection.

I. INTRODUCTION

X-Rays are forms of radiant energy, like light or radio waves. Unlike light, X-Rays can penetrate the body, which allows a radiologist to produce pictures of internal structures. They are oldest, cheapest method for obtaining information about many types of diseases and fractures [8 ,9]. It is a noninvasive medical test that helps physicians diagnose and treat medical conditions.

Gray scale is a range of monochromatic shades from black to white. So a grayscale image contains only shades of gray and no color. They are different from black and white images. Their pixel value ranges from 0 to 255 [6, 14]. They have only intensity values. Gray scale images are made up of only one bit value. They lack the chromatic information [10].

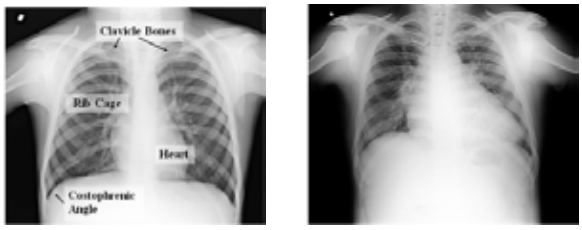

Fig. 1. Chest X-Ray Images

1.1 Related Research in Lung Boundary Segmentation

Over the past decade, a number of research groups have worked on chest X-ray analysis, and various methods have been proposed for lung boundary segmentation. Sema Candemir, Stefan Jaeger, et al. [11] has proposed Segmentation approach in Lung X-Ray images. The lungs in their nature are segmented into five lobes. The lobes of the lung are further divided into segments which physicians based on to define in which lobe the lesion is localized when they use chest radiographies.

B. Ginneken and B. Romeny, has proposed "Automatic segmentation of lung fields in chest radiographs," This work presents the automatic segmentation of lung fields in chest radiographs and develops the rule based scheme to detect the lung contours. This algorithm is compared to several pixel classifiers using different combinations of features. Savitha S. K, Aprameya K. S, Alwyn R. Pais has proposed "An Efficient Learning Based Algorithm For Lung Boundary Detection For Chest X-Ray Images". This work presents the lung boundary detection in chest X-Ray images using the learning algorithm. Sudha.V, Jayashree.P has proposed "Lung Nodule Detection in CT Images Using Thresholding and Morphological Operations". This paper presents the lung nodule detection in CT images using thresholding and morphological operators. This method has two stages: lung region segmentation through thresholding and then segmenting the lung nodules through thresholding and morphological operations. According to Donia Ben Hassen, Hassen Taleb, in article titled "A Fuzzy Approach to Chest Radiography Segmentation involving Spatial Relations. The results demonstrate that the introduction of spatial relations can improve the recognition and segmentation of structures with low contrast and ill-defined boundaries and its surroundings

1.2 System Overview and Contribution

In existing method the rule-based segmentation methods contain sequences of steps and rules such as thresholding or morphological operations. They mainly model the intensities of inside and outside of the lung regions, and classify the image pixels into either object. Active shape models (ASM) and active appearance models (AAM) applied to lung region segmentation [11 ,13].

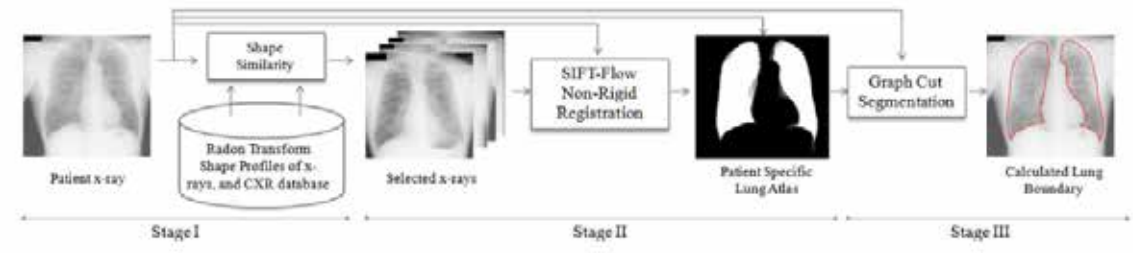

Fig. 2. Idea for Lung Boundary Segmentation

To avoid this problems this research proposed the random transform shape similarity. The content based image retrieval approach is used for the similarity. In feature extraction use the SIFT flow and deformable wrapping for the input image. The segmentation process use the graph cut algorithm.

II MODULES

The paper consists of the following modules,

1. Input X-ray
2. Find the shape similarity for the CXR database using CBIR
3. SIFT Flow Non-Rigid Registration
4. Graph cut Segmentation
5. Find Lung Boundary

The segmentation of Lung boundary consists of the following architecture.

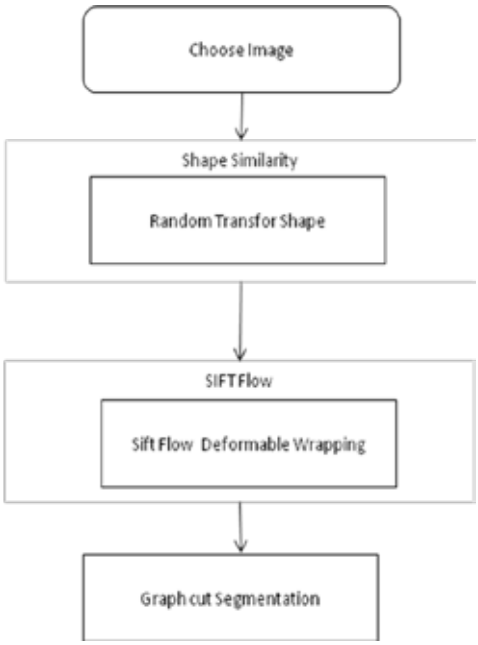

Fig. 3. System Architecture

2.1 Shape Similarity for CXR database Using CBIR

First identify a small subset of images in the training database. This subset of training images develops the patient specific lung model using CBIR. CBIR system is used to produce a ranked subset of images most similar to the query which in our case is a new patient CXR image. The CXR database is pre-processed and consists of globally aligned and normalized CXRs. The Radon transforms or orthogonal projection profiles are to compare and rank the similarity between two patient's lung images. The Radon transform projection along an arbitrary line in the x-y plane is defined as

$$R(\rho,\theta) = \iint I(x,y)\delta(\rho - x\cos\theta - y\sin\theta)dx\,dy$$

The Radon transform computes a projection of the image as a sum of line integrals accumulating pixel intensities. The partial Radon transform projection method is fast to compute and only an approximate matching atlas set of lung segmentations from the CXR database is needed to compute a spatial prior that can be refined in the subsequent phase of the algorithm. First calculate the intensity projection of the histogram-equalized images in

the vertical and the horizontal directions. Then measure the similarity of each projection profile between the atlas database and the patient chest X-ray using the average Bhattacharyya coefficient.

$$\mathrm{BC}(I_1, I_2) = \alpha \sum_{x=1}^{n} \sqrt{p_1(x)p_2(x)} + (1-\alpha) \sum_{y=1}^{m} \sqrt{q_1(y)q_2(y)}$$

To select a set of best fit training atlases from the anatomical database, segmented lung images are used by learning a patient specific lung model. The registration performance is significantly improved when a personalized lung model is designed by comparing the patient X-ray with pre-segmented lung images in the CXR database using a fast shape similarity measure based on partial Radon transforms.

2.2 SIFT Flow non-rigid Registration

The SIFT features of the X-rays are calculated as follows. First, the gradient orientations and magnitudes are computed at each pixel. The gradients are weighted by a Gaussian pyramid. The regions are subdivided into quadrants. In each quadrant, a gradient orientation histogram is formed by adding the gradient values to one of eight orientation histogram bins.

The concatenation of orientation histograms of the quadrants form the SIFT descriptor vector are obtained from the center pixel of the region. Once calculation of the SIFT features for the image pair, the registration algorithm computes pixel-to-pixel correspondences by matching the SIFT descriptors.

1. The SIFT-flow algorithm calculates corresponding matches for each pixel of these X-ray pair by solving the flow vectors.
2. Colored markers indicate corresponding matches for a few pixel samples.
3. The lung boundary in one X-ray image approximately matches the lung boundary in the other X-ray.
4. The spatial shifts between corresponding matches define the transformation mapping for pixels.
5. The algorithm applies the transformation mapping by simply shifting each pixel in the training mask according to the calculated shift distance.
6. The registration stage is repeated for each of the top- similar X-rays to the patient X-ray.
7. The lung model for the patient X-ray is built-up using the mean of the top-ranked registered masks.
8. The computed patient specific lung model is a probabilistic shape prior.

2.3 SIFT Features Extraction

Scale-invariant feature transform (or SIFT) is an algorithm in computer vision to detect and describe local features in images [5,13]. Applications include object recognition, robotic mapping and navigation, image stitching, 3D modeling, gesture recognition, video tracking, individual identification of wildlife and match moving. SIFT key points of objects are first extracted from a set of reference images and stored in a database. An object is recognized in a new image by individually comparing each feature from the new image to this database and finding candidate matching features based on Euclidean distance of their feature vectors [5, 6].

From the full set of matches, subsets of key points that agree on the object and its location, scale, and orientation in the new image are identified to filter out good matches. The determination of consistent clusters is performed rapidly by using an efficient hash table implementation of the generalized Hough transform [1]. Each cluster of 3 or more features that agree on an object and its pose is then subject to further detailed model verification and subsequently outliers are discarded. The SIFT features are local and based on the appearance of the object at

particular interest points, and are invariant to image scale and rotation. They are also robust to changes in illumination, noise, and minor changes in viewpoint [2]. In addition to these properties, they are highly distinctive, relatively easy to extract and allow for correct object identification with low probability of mismatch.

Algorithm:

1. Scale Space Extrema Detection:

· This stage of the filtering attempts to identify those locations and scales those are identifiable from different views of the same object.

· To locating scale-space extrema, D(x, y, σ) by computing the difference between two images, one with scale k times the other. D(x, y, σ) is given by:

$$\mathbf{D(x, y, \sigma) = L(x, y, k\sigma) - L(x, y, \sigma)}$$

· To detect the local maxima and minima of D(x, y, σ) each point is compared with its 8 neighbors at the same scale, and its 9 neighbors up and down one scale.

· If this value is the minimum or maximum of all these points then this point is an extrema.

2. Key point Localization - To improve Key points and throw out bad once
3. Orientation Assignment - To remove the effects of rotation and scales
4. Create Descriptor - Using the histograms for orientation

2.4 Graph Cut Segmentation

The graph cuts algorithm models computer vision problems using an undirected graph G = (V,E). The set of vertices V represents the pixel properties such as intensity; and the set of edges E connects these vertices. Graph cuts can be employed to efficiently solve a wide variety of low-level computer vision problems such as image smoothing, the stereo correspondence problem, and many other computer vision problems that can be formulated in terms of energy minimization [12]. Under most formulations of such problems in computer vision, the minimum energy solution corresponds to the maximum a posteriori estimate of a solution. It involves cutting a graph the term "graph cuts" is applied specifically to those models which employ a max-flow/min-cut optimization.

Algorithm:

1. Consider set of labels and set of sites.
2. In each site assign the label.
3. Energy Minimization is followed

$$E(f) = \sum_{p \in S} D_p(f_p) + \lambda \sum_{(p,q) \in \mathcal{N}} \omega_{pq} \cdot T(f_p \neq f_q)$$

4. In image segmentation it is expected the boundary to be positioned on the edges.

$$\omega_{pq} = e^{-\frac{(I_p - I_q)^2}{2\delta^2}} \cdot \frac{1}{dist(p,q)}$$

III EVALUATION METRICS

In order to compare segmentation quality with the segmentation performances in the literature, the existing work on this segmentation used three commonly used metrics [3 ,7].

1) The Jaccard Similarity Coefficient (overlap measure):

It is the agreement between the ground truth (GT) and the estimated segmentation mask (S) over all pixels in the

$$\Omega = \frac{|S \cap GT|}{|S \cup GT|} = \frac{|TP|}{|FP| + |TP| + |FN|}$$

image.

Where TP (true positives) represents correctly classified pixels, FP (false positives) represents pixels that are classified as object but that are in fact background, and FN (false negatives) represents pixels that are classified as background.

2) Dice's Coefficient

It is the overlap between the ground truth GT and the calculated segmentation mask S,

$$DSC = \frac{|S \cap GT|}{|S| + |GT|} = \frac{2|TP|}{2|TP| + |FN| + |FP|}.$$

3) Average Contour Distance (ACD)

It is the average distance between the segmentation boundary S and the ground truth boundary GT. Let ai and bj be the points on the boundary S and GT, respectively [4]. The minimum distance of point ai on S to the GT boundary is defined as follows:

$$d(a_i, GT) = \min_j \|b_j - a_i\|.$$

For ACD computation, the minimum distance for each point on the boundary S to the contour GT is computed. Then, the distances are averaged over all points of boundary. In order to make the similarity measure symmetric, the computation is repeated from contour GT to contour S,

$$ACD(S, GT) = \frac{1}{2}\left(\frac{\sum_i d(a_i, GT)}{|\{a_i\}|} + \frac{\sum_j d(b_j, S)}{|\{b_j\}|}\right)$$

The SIFT-flow algorithm computes correspondences between the patient and the training X-rays. The spatial distances between the corresponding matches are given by the transformation mapping between the pixels. In order to show the visual success of the registration stage, the image is warped the training images with the calculated transformations [15].

IV EXPEREMENTAL RESULTS

The results are evaluated using MATLAB and displayed in GUI environment. After choosing the image from the dataset, the shape similarity has to be done with the existing dataset.

Fig. 4. Shape Similarity

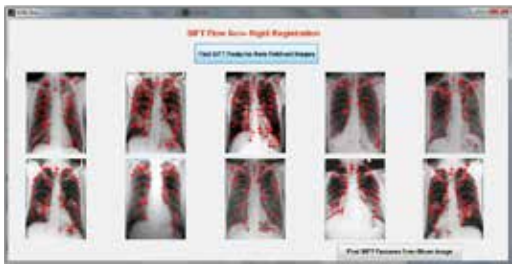

Fig.5 SIFT Flow Non-Rigid Module Images

Fig.6 SIFT Flow Non-Rigid Registration Module Images

Fig.7 Graph Cut Segmentation

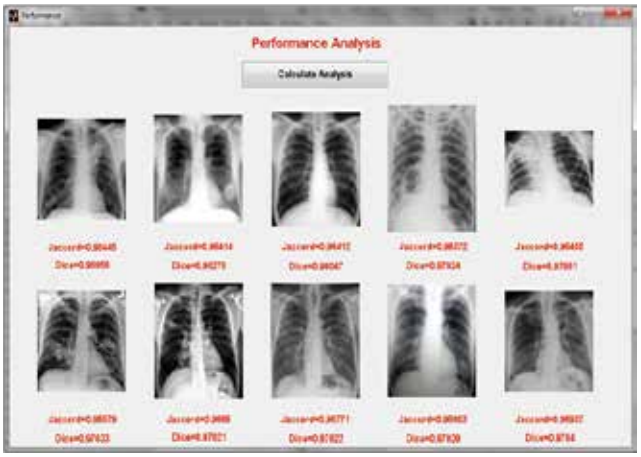

Fig 8.Performance Analysis

V CONCLUSION

This work successfully proposed lung segmentation in chest radiograph images. The shape similarity used the random transform shape. In feature extraction it used the SIFT features. And the SIFT flow deformable wrapping for given input image. Finally applied the graph cut segmentation used for the lung boundary detection. In earlier approach the accuracy rate was 95.4%. By combining the Integral values this work increase the accuracy level by still optimizing the graph cut values and finalized by 97.4%. This research work will help the Doctors to identify the severity of the infection with the chest X-Ray image itself, instead of going for other expensive diagnosis tests.

VI FUTURE ENHANCEMENT

This Research work is carried out for the detection of Tuberculosis infection in chest X-Ray images. This can be further improved with other types of abnormal symptoms in chest X-Ray which includes, Collapsed lung, Collection of fluid around the lung, Lung cancer, Lung tumor, Malformation of the blood vessels, Scarring of lung tissue, Pneumonia.

REFERENCE

[1] Asem M. Ali Ayman S. El-Baz Aly A. Farag “A NOVEL FRAMEWORK FOR ACCURATE LUNG SEGMENTATION USING GRAPH CUTS” Feb 2007 IEEE Transaction on Image Processing.

[2] Gomathi M, Dr. P.Thangaraj, " A New Approach to Lung Image Segmentation using Fuzzy Possibilistic C-Means Algorithm", International Journal of Computer Science and Information Security, Vol. 7, No. 3, March 2010

[3] B. Ginneken and B. Romeny, “Automatic segmentation of lung fields in chest radiographs,” Med. Phys., vol. 27, no. 10, pp. 2445–2455, 2000.

[4] Herve Lombaert Yiyong Sun Leo Grady Chenyang Xu “A Multilevel Banded Graph Cuts Method for Fast Image Segmentation” Proceedings of the ”Tenth IEEE International Conference on Computer Vision”, ICCV 2005 Volume 1, pp. 259.

[5] Keita Nakagom, Akinobu Shimizu, Hidefumi Kobatake, Masahiro Yakami, Koji Fujimoto, Kaori Togashi “Multi-shape graph-cuts and its application to lung segmentation from a chest CT volume” Fourth International Workshop on Pulmonary Image Analysis.

[6] Lung information, http://www.radiologymasterclass.co.uk

[7] Ravia Shabnam Parveen N, Dr. M.Mohamed Sathik, "Enhancement of Bone Fracture Images by Equalization Methods", International Conference on Graphics and Image Processing and Published by IEEE Computer Society with ISBN 978-0-7695-3892-1, Kota Kinabalu, MALAYSIA, from 13-11-09 to 15-11-09.

[8] Ravia Shabnam Parveen N, Dr. M.Mohamed Sathik, "Segmenting the Colored X-Ray Images", International Conference on Computer Applications, Pondicherry, from 24-12-10 To 27-12-10.

[9] Ravia Shabnam Parveen N, Dr. M.Mohamed Sathik, "Detection of Pneumonia in Chest X-Ray Images", International Journal of X-Ray Science and Technology with ISSN : 0895-3996, (Scopus Indexed Journal), Volume 19, Number 4, 2011.

[10] Savitha S. K, Aprameya K. S, Alwyn R. Pais "AN EFFICIENT LEARNING BASED ALGORITHM FOR LUNG BOUNDARY DETECTION FOR CHEST X-RAY IMAGES" International Journal of Emerging Trends & Technology in Computer Science (IJETTCS) Volume 3, Issue 4, July-August 2014.

[11] Sema Candemir, Stefan Jaeger, Kannappan Palaniappan, Jonathan P. Musco, Rahul K. Singh, Zhiyun Xue, Alexandros Karargyris, Sameer Antani, George Thoma, and Clement J. McDonaldLung has proposed "Segmentation in Chest Radiographs Using Anatomical Atlases With Nonrigid Registration", IEEE TRANSACTIONS ON MEDICAL IMAGING, VOL. 33, NO. 2, FEB 2014.

[12] Sema Candemir, Stefan Jaeger, Kannappan Palaniappan, Sameer Antani, and George Thoma "Graph Cut Based Automatic Lung Boundary Detection in Chest Radiographs" 1st Annual IEEE Healthcare Innovation Conference of the IEEE EMBS Houston, Texas USA, 7 - 9 November, 2012.

[13] Sudha.V, Jayashree.P "Lung Nodule Detection in CT Images Using Thresholding and Morphological Operations" International Journal of Emerging Science and Engineering (IJESE) ISSN: 2319–6378, Volume-1, Issue-2, December 2012.

[14] X-Ray information on safety, Radiologyinfo.org.

[15] Zhennan Yan, Jing Zhang, Shaoting Zhang, and Dimitris N. Metaxas, "Automatic Rapid Segmentation of Human Lung from 2D Chest X-Ray Images".

AUTHOR:

Dr. N.Ravia Shabnam Parveen, is working as Assistant Professor (Selection Grade), in the Department of MCA, K.L.N. College of Engineering, Madurai. She has completed her MCA in Fatima College, Madurai and M.Phil, Computer Scienec in Madurai Kamaraj University College, Madurai. She has Completed Ph.D from Bharathiar University, Coimbatore. She has presented many Research papers in International & National conferences and Journals. Her area of specialization is Image Processing. Currently doing M.E in Computer science.

FUZZY LOGIC BASED REGION WISE ROUTING PROTOCOL FOR WIRELESS SENSOR NETWORK

Mugdhita Rege[1], P. P. Narwade[2]

[1]PG Student, MGM College of Engineering and Technology Kamothe, (India)

[2]Professor, Dept. Electronics and Telecommunication Engg MGM College of Engineering and Technology Kamothe, (India)

ABSTRACT

Wireless sensor networks are collection of several small, battery operated electronic devices known as sensors in order to monitor physical phenomenon such as temperature, pressure or humidity. Furthermore these sensor nodes are usually operated by battery which is normally not easy to replace. Till now many routing protocols have been proposed for energy efficiency of both homogeneous and heterogeneous environments. Hierarchical routing protocols are considered as best in regard to energy efficiency [1]. Clustering technique using hierarchical routing protocols minimizes energy consumption in a great extent. We propose here a protocol designed for the characteristics of heterogeneous WSNs. Region-wise routing protocol (FUZZY-SEP) is used for some nodes to transmit data directly to base station. In FUZZY-SEP, Cluster Head (CH) selection is based on fuzzy level information which minimizes the time for the selection of cluster head.

Keywords*: *Wsn (Wireless Sensor Network), Fuzzy-Sep (Region-Wise Routing Protocol), Ch (Cluster Head), Bs (Base Station), Fuzzy Logic, Network Lifetime, Routing, Energy Efficiency

I. INTRODUCTION

Wireless sensor network (WSN) has appeared as an emerging field in last few years providing a variety of useful applications such as target detection and monitoring, scientific observation, safety-related. The purpose of mapping a WSN is to collect relevant data for processing and reporting. Sensor nodes periodically sense the environment and transmit the data with respect to time [2]. The occurrence of a certain event can be recognized from a sudden drastic changes sensed by wireless sensor network. Sensor nodes are battery-operated and are expected to operate for a long time without any failure. But reality is different from our expectations as it is difficult rather impossible to replace the battery of sensor nodes .Thus energy consumption is a major key objective in wireless sensor network communication. By varying the parameters like distance, residual energy and load we can prolong the network lifetime which in turn leads to reduced energy consumption [3]

Wireless sensor network is formed by number of identical nodes. A sensor node is composed of sensor unit, analog-digital circuitry, processor, memory, transceiver, battery source and a set of protocols to support the communication. These nodes are responsible for data gathering which is carried on in order as shown in fig. 1 - sensing, processing and communication. The sensor nodes are usually programmed to monitor or collect data from surrounding environment and pass the information to the sink [4].To maintain the connectivity and coverage among all the nodes in the network, proper routing algorithm is essential.

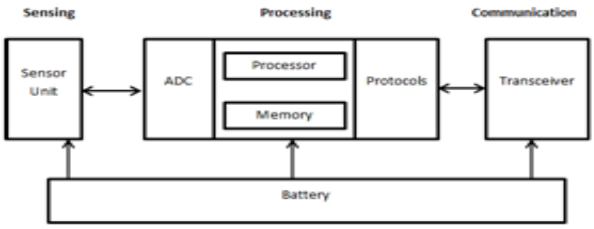

Fig. 1- Components of a sensor node

All the recent research work focuses on sensor networks that are based on clustering technique. Grouping of sensor node is called as cluster. Clustering provides WSNs large coverage area and network scalability. Clusters create hierarchical fashion which enables network to use resources efficiently. In hierarchical clustering single cluster head (CH) is elected in a single cluster which transmits data to the sink node. Clustering is classified as Homogeneous or Heterogeneous. Homogeneous clustering consists of identical sensors which are equally capable of sensing, computation, communication, and possess equal energy level. This type of identical sensor networks is termed as Homogeneous. Whereas, the possibility of working with more than one type of sensors within a same network is mentioned as Heterogeneous. Heterogeneous networks use nodes with different battery and different functionalities [5]. The Low Energy Adaptive Clustering hierarchy protocol (LEACH) is first and most basic hierarchical clustering algorithm which is popular for energy efficiency and reduced power consumption. A cluster head (CH) is responsible for coordinating the transmission of data between the BS and other sensor nodes. Each node elects itself as a cluster head based on the probability scheme and realizes its availability to other sensor nodes in the cluster as shown in fig 2. In clustering technique apart from residual energy distance is another major attribute to determine the signal strength [6].

A routing protocol is a protocol that specifies how sensor nodes communicate with each other [7]. To send data between sensor nodes and the base stations routing is essential. It builds the path between source and destination and maintains it during network utilization.

Routing protocols can be classified as based on their functionality and applications as proactive, reactive and hybrid. In a proactive protocol data is transmitted or routed via a predefined route when the sensor nodes sense the environment and thereafter data is transmitted to a BS. Whereas in a reactive protocol when some sudden changes are the sensed i.e. when the sensed data cross pre-determined threshold value, the nodes immediately react. And hybrid protocol inhere the characteristics of both proactive and reactive protocols. The Low Energy Adaptive Clustering hierarchy protocol (LEACH) utilizes this type of protocol. The Threshold sensitive Energy Efficient sensor Network (TEEN) is an example of a reactive protocol. The best example of hybrid protocol is Adaptive periodic Threshold sensitive Energy Efficient sensor Network (APTEEN) that incorporates both proactive and reactive concepts [6].

Wireless sensor network is composed of number of sensor nodes which are uniformly distributed all over the network and a single sink node. The position of the sink node can be arbitrary. Transmission between adjacent cell are carried out at same power level.

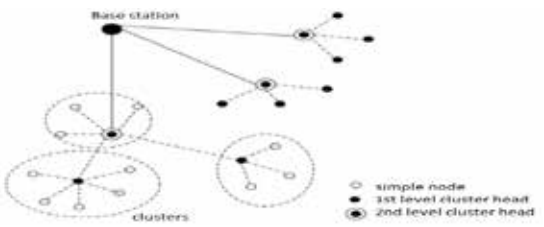

Fig.2- Clustering process in WSN

Routing is done among the nodes i.e. each cell forwards its packets to the cell that is closest to the sink node; upon reaching the closest node the packet is routed to the sink node [8].

II. DESIGN ISSUES

A network should be designed by keeping in mind network characteristics and challenging parameters that appear while designing a network. Thus we can evaluate a performance of a network on following basis:

(i.) ***Power source****:* Sensor nodes are powered by battery-source which have limited energy. If the energy of sensor nodes crosses certain threshold level the sensor becomes faulty. In such cases they are difficult to replace as the nodes are employed in some hostile or adverse areas.

(ii.) ***Stability Period:*** The period in which the network starts its operation till the death of the first node is stability period. It is also referred to as "stable region or steady state".

(iii.) ***Instability Period:*** The period of timefrom the death of the first node until the death of the last node is instability period. It is referred as unstable region.

(iv.) ***Network life time:*** It is the time interval between stability and instability period:

Network lifetime = Stability Period + Instability Period

(v.) ***Alive Nodes:*** It is the total number of normal nodes having energy greater than zero i.e. alive.

(vi.) ***Throughput:*** It is the total rate of data sent over the network from nodes to their respective CHs and from CHs to base station [3], [6].

In remote sensor system, it is important to foresee the energy level of the framework. In this manner an energy model is characterized for energy examination of a sensor system. We accept that all nodes are consistently circulated everywhere throughout the system in progressive hierarchical groups. What's more a small amount of the aggregate nodes are furnished with more energy. Let m be division of the aggregate nodes n, which are furnished with α time more energy than alternate nodes. We mention these nodes as super nodes, (1-m)×n are ordinary nodes. Presently the election of cluster head (CH) is done in each round so the load is decently adjusted among all nodes. The cluster head then needs to report the sink node [3],[9]. The energy model is illustrated in fig. An essential outline issue in sensor systems is energy productivity.

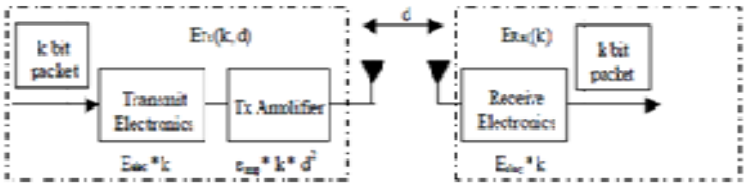

Fig.3 – Radio Energy Model [9]

Energy utilization for accumulation of information is substantially less when contrasted with energy utilized as a part of information transmission.Thus, to transmit a k-bit message, a separation d, the radio uses:

$$ETx(k,d) = ETx - elec(k) + ETx - amp(k,d)$$
$$= Eelec*k + eamp*k*d_2$$

and to receive this message, the radio uses:

$$ERx(k) = ERx - elec(k)$$
$$= Eelec*k$$

III. PROBLEM DESCRIPTION

For an energy proficient operation, ideal cluster arrangement is important to guarantee that energy is devoured at an adjusted rate. The operation of group based WSNs is broken into rounds. Each round is comprised of cluster head choice, cluster development and information transmission. The system lifetime is the quantity of rounds in which all nodes have non-zero energy. The majority of the grouping calculation depends on an irregular number created by every sensor node in every round for the procedure of cluster head selection. Late studies demonstrates that if parameters like residual energy, distance to base station and centrality are considered at the time of cluster head election, system execution can further be progressed. In this reference this exploration work is dedicated towards execution advancement of region-wise routing protocol and fuzzy logic.

IV. PROPOSED METHOD

We propose a Region-wise routing protocol (FUZZY-SEP) with joint consideration of cluster head selection and routing discovery. In SEP protocol ordinary nodes and super nodes are sent randomly; If greater part of typical nodes are conveyed far from base station it expends more energy while transmitting information which brings about the shortening of strength period and abatement in throughput. Consequently proficiency of SEP declines. To evacuate these defects we partition system field in small regions. Since corners are most far off regions in the field, where nodes require more energy to transmit information to base station. So in fuzzy-SEP, ordinary nodes are put close to the base station and they transmit their information straightforwardly to base station. However super nodes are put far from base station as they have more energy. On the off chance that super nodes transmit information specifically to base station more energy expends, so to spare energy of super nodes grouping procedure is utilized for super nodes only. The most important part of the proposed method is Fuzzy Inference System (FIS). The FIS has four parts and the architecture of the model is shown in fig. 4

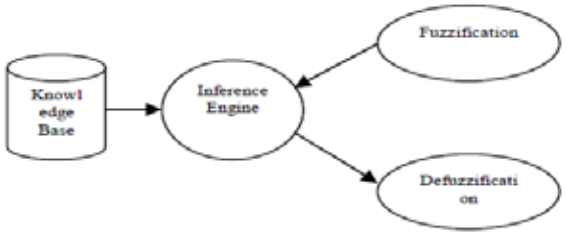

Fig.4 – Fuzzy Inference System Architecture

(i.) ***Fuzzification module:*** System inputs, which are fresh numbers, are changed into fuzzy sets by applying a fuzzification capacity.

(ii.) ***Knowledge base:*** It stores IF-THEN standards.

(iii.) ***Inference Engine:*** By making fuzzy guessing on the inputs and IF-THEN principles it mimics the human thinking methodology.

(iv.) ***Defuzzification module:*** The fuzzy set acquired by the inference tool is changed into a crisp values.

4.1 Region-Wise Routing Protocol

Region-wise routing protocols join features of both proactive and reactive ones. Ordinarily, the topology is separated into specified regions or zones. FUZZY-SEP is a mixture protocol that divides the system into a few zones, which makes a various leveled protocol as the ZRP protocol (zone-routing protocol). FUZZY-SEP is in

light of GPS (Global positioning system), which permits every node to recognize its physical position before mapping a location with table to distinguish it to which it belongs [5].

4.2 Fuzzy Logic Algorithm

Fuzzy Logic is a numerical control method to express human thinking in thorough scientific documentation. Not at all like traditional thinking in which, a recommendation is either true or false, fuzzy logic creates truth estimation of a suggestion taking into account phonetic variables and derivation rules. It has the beneficial points of simple usage, robustness, and capacity to be estimated to any nonlinear mapping. In fuzzy frameworks, the dynamic conduct of a framework is described by a set of semantic fuzzy principles in view of a human expert. These rules are the main center of attraction of a fuzzy framework and may be given by specialists or can be separated from numerical information [2], [4]. In either case, the standards that we are keen on can be communicated as an accumulation of IF-THEN articulations (IF predecessors THEN consequents). Predecessors and consequents of a fuzzy rule structure create the fuzzy input space and fuzzy yield space separately is characterized by blends of fuzzy sets. We suggest here the IF-THEN rule set designed for fuzzy-SEP protocol.
The process of Cluster Head selection consists of distance, residual energy and load of a super node. Following table uses three membership functions to show the various degrees of input variables.

Input	Membership		
Distance to the BS	Reachable	Considerable	Far
Residual Energy	Low	Adequate	High
Load	Less	Medium	Heavy

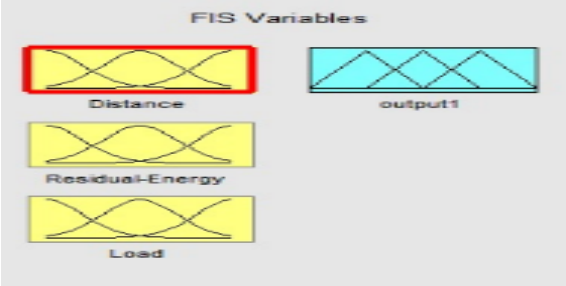

Fig.5–Output Function Depending Upon Three Inputs

V. SIMULATION

Simulation by using MATLAB software will give brief idea about this energy efficient technique. Here consider the MATLAB simulation results. Consider field dimensions in x and y directions to be 100 meters. The total numbers of nodes are assumed to be 100 with 10% probability to become a cluster head. Initial energy of the energy model is 0.5. The performance is evaluated for 5000 number of rounds and the result of FUZZY-SEP is shown as follows:

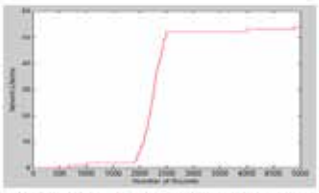

Fig.6 – Network Lifetime Vs. number of rounds for FUZZY-SEP

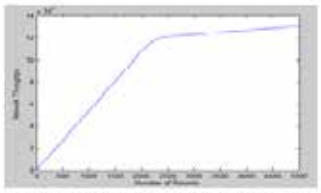

Fig.7 – Network throughput Vs. number of rounds for FUZZY-SEP

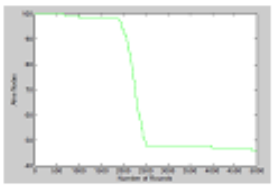

Fig.8 – Alive nodes Vs. number of rounds for FUZZY-SEP

VI. CONCLUSION

The proposed protocol uses the fuzzy data for the choice of cluster head to reduce the time consumed for cluster head election. To address problem of energy efficiency, we have designed FUZZY-SEP protocol implementing fuzzy logic, and presented our approach via a simulation study. This method minimizes overall utilization of energy in course while cluster head election process. So it prolongs the lifetime of system. The hierarchical clustering and organization of the nodes in diverse locations depending upon their energy level optimizes the stability period and throughput of the system.

REFERENCES

[1.] Sonam Maurya, "Hybrid Routing Approach for Heterogeneous Wireless Sensor Networks using Fuzzy Logic Technique" , Fourth International Conference on Advanced Computing & Communication Technologies, 2014

[2.] Byoung-Dai Lee and Kwang-Ho Lim, "An Energy-Efficient Hybrid Data-Gathering Protocol Based on the Dynamic Switching of Reporting Schemes in Wireless Sensor Networks", IEEE SYSTEMS JOURNAL, VOL. 6, NO. 3, SEPTEMBER 2012

[3.] Imad S. AlShawi , "Lifetime Enhancement in Wireless Sensor Networks Using Fuzzy Approach and A-Star Algorithm", IEEE SENSORS JOURNAL, VOL. 12, NO. 10, OCTOBER 2012

[4.] Imad S. AlShawi, "A Fuzzy-Gossip Routing Protocol for an Energy Efficient Wireless Sensor Networks", IEEE 2012

[5.] Badr CHAHIDI, "Hybrid Routing Protocol For wireless sensor networks", IJCSI International Journal of Computer Science Issues, Vol. 9, 2012

[6.] Gaurav Sharma and Ravi R. Mazumdar ,"A Case for Hybrid Sensor Networks", IEEE/ACM TRANSACTIONS ON NETWORKING, VOL. 16, NO. 5, OCTOBER 2008

[7.] Shio Kumar Singh, "Routing Protocols in Wireless Sensor Networks – A Survey", International Journal of Computer Science & Engineering Survey (IJCSES) Vol.1, No.2, November 2010

[8.] Vinay Kumar, "A Review Study of Hierarchical Clustering Algorithms for Wireless Sensor Networks", IJCSI International Journal of Computer Science Issues, Vol. 11, Issue 3, No 1, May 2014.

[9.] Debnath Bhattacharyya, "A Comparative Study of Wireless Sensor Networks and Their Routing Protocols", Journal ofSensors2010

LOW COST MOBILE SHOE FOR PATIENTS WITH PARALYZED LEG

D.Selvaraj[1], D.Arul Kumar[2], D.Dhinakaran[3]

[1]*Associate Professor, Department of ECE, Panimalar Engineering College, Tamilnadu, (India)*

[2]*Assistant Professor, Department of ECE, Panimalar Institute of Technolog, Tamilnadu,(India)*

[3]*Assistant Professor, Department of CSE, Peri Institute of Technology, Tamilnadu, (India)*

ABSTRACT

The main aim of this project is to make the paralyzed leg into movable leg. This proposed system is especially for the persons having single paralyzed leg. Here a shoe is designed to operate in free living conditions. The principle behind this is light sensing and moving to appropriate distance. Let we consider a handicap person who has his right leg paralyzed and his left leg perfectly normal. In this project a self moving shoe with wheels for the right leg and a normal shoe for the left leg will be designed. When the person is standing with his legs together, there is a continuous passage of light from the light source to the light detector from one shoe to another. At that time there is no need of controlling or driving the wheel of paralyzed leg. When the person keeps his left leg forward, in an attempt to walk forward, there is a break in the passage of light between the shoes. At that time, microcontroller detects the variation and make the motor fitted in the paralyzed leg will run or move until it reaches the normal leg (i.e., by detecting the source). Therefore, the right shoe, provided with wheels moves forward to reach the light from the left shoe, to come in parallel position with the left shoe. Likewise, for every step the person keeps with his left leg, the right shoe helps the person move his leg to appropriate distances. Therefore, the person with a paralyzed leg is able to walk with the walking shoe.

***Keywords:* Mobile Shoe, Monoplegia, Paralysis, Paralyzed Leg, Wearable Shoe**

I. INTRODUCTION

Paralysis is defined as complete loss of strength in an affected limb or muscle group. Thousands of people every year suffer spinals and lose their ability to walk. Complete loss of communication prevents any willed movement at all. This lack of control is called paralysis. [1]. the types of paralysis are classified by region:

- monoplegia, affecting only one limb
- diplegia, affecting the same body region on both sides of the body
- hemiplegic, affecting one side of the body
- Paraplegia, affecting both legs and the trunk.

The nerve damage that causes paralysis may be in the brain or spinal cord (the central nervous system) or it may be in the nerves outside the spinal cord (the peripheral nervous system). The most common causes of damage to the brain are,

- stroke, tumor, trauma (caused by a fall or a blow), multiple sclerosis (a disease that destroys the protective sheath covering nerve cells)[2]
- cerebral palsy (a condition caused by a defect or injury to the brain that occurs at or shortly after birth)
- metabolic disorder (a disorder that interferes with the body's ability to maintain itself)

Solitaire Revascularization Device is a mechanical thrombectomy device combining the ability to restore blood flow, administer medical therapy, and retrieve clot in patients experiencing acute paralysis. Mechanically breaks up and removes the blood clot. It needs optimal radial force and the uses of medical therapy.The drawback of these devices are, 1) these technology needs very high investment to cure the problem which is very difficult for the poor people [3]. 2) The person for whom the paralysis cannot be cured or the poor people having paralysis will go for a walking stick or a wheel chair. (i.e. dependency).

In our proposed method, a new type of mobile shoe which is based on light sensing is proposed. This shoe helps the monoplegia patient (i.e., paralysis affecting only one limb) to walk with the affected leg as like a normal leg [4]. This shoe can be implemented at very low cost suitable to all kinds of people and make the patients to feel independent.

The paper is organised as follows, the construction and working of the proposed model is presented in section 2. The detailed experimental results and discussions are given in section 3. The conclusions are summed up in section 4.

II. CONSTRUCTION AND WORKING

2.1 Basic Principle

The main principle needed for constructing our project is light sensing and detection .It includes light sensor at transmission side and light detector at the receiving side. Laser is used for light sensing which is given at the normal leg shoe and LDR is used for light detecting which is given at the affected leg shoe.LDR at the receiving side detects the laser light , thereby it helps the person to move his affected leg forward until it reaches the normal leg.

2.2 Block diagram

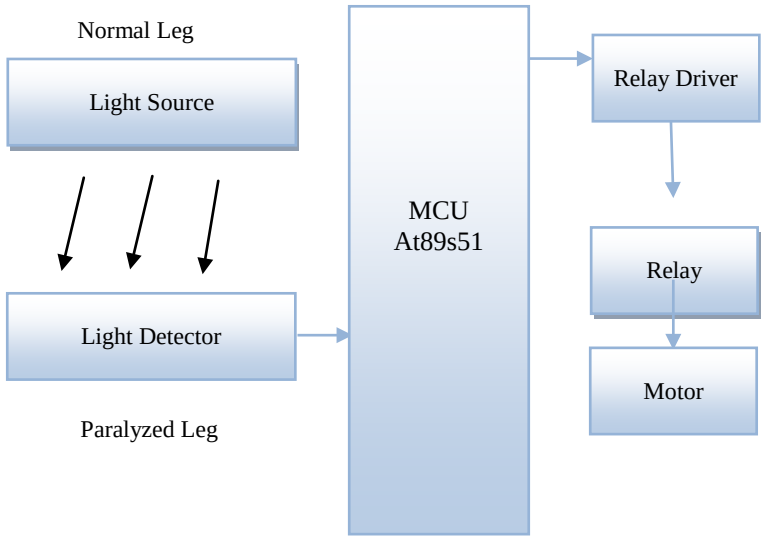

Fig. 1: Block diagram of light sensing mobile shoe

The block diagram mainly contains two sections namely transmitting section and the receiving section as shown in Fig. 1. Transmitter is placed at the normal leg. Receiver is placed at the affected leg. LASER light is used for transmitting light to the receiver. LDR is used for receiving the LASER light which is at the receiving side. LDR transmit the received signal to the 89s51 microcontroller. From the controller the signal is given to the relay driver. Relay driver drives the relay so that it delivers the input for the motor to move the affected leg.

2.3 Working

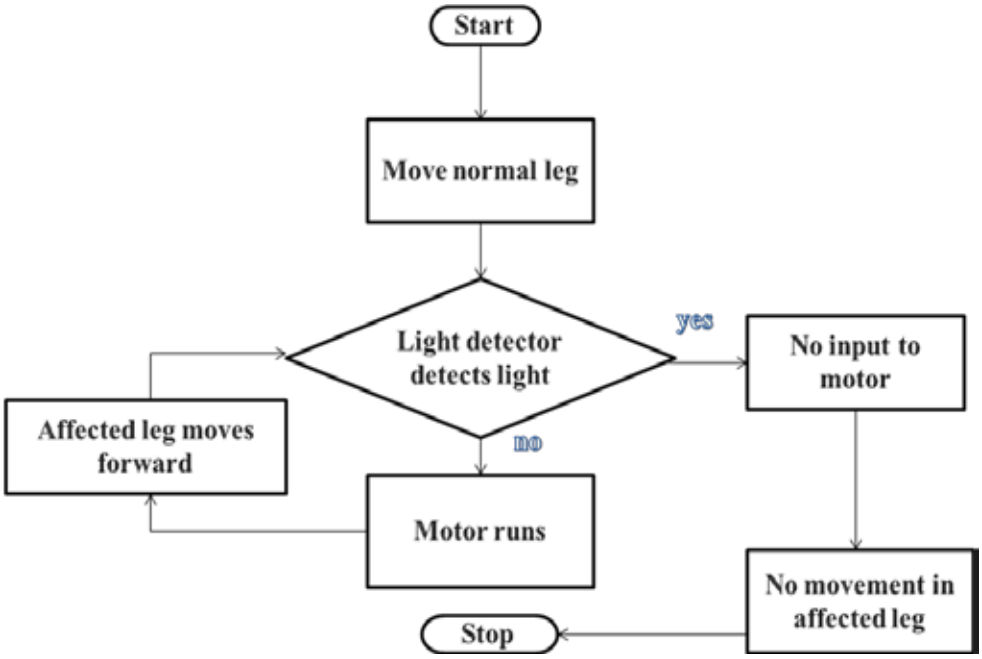

Fig. 2: Flowchart of Mobile Sensing Shoe

The working operation can be explained in two stages namely,

a) When the person is not moving.

b) When the person step forward his normal leg.

When the person was standing (i.e., before moving his normal leg forward) LASER light source given to the transmitter placed at the normal leg continuously transmit the light to the LDR placed at the affected leg. There will be a continuous passage of light between the normal leg and the affected leg. At that time micro controller make the relay to go low whenever the LDR is high. Since the relay was low there will be no input for the motor to move the affected leg forward.

When the person step forward his normal leg, LDR at the affected leg is unable to receive the LASER light which is in normal leg. That time there will be a breakage in the continuous passage of light which cause the LDR to goes low. Microcontroller allows the relay to go high whenever the LDR is low. Relay driver is able to drive the high input relay. Thus the relay supplies the required input for the motor to run. Finally motor runs the wheels attached to the affected leg and helps the patient to move his affected leg forward until it reach the normal leg.(i.e., until there is a continuous passage of light between normal leg and the affected leg.

III. EXPERIMENTAL RESULTS

The snap shots of the prototype of our proposed mobile shoe are shown in Fig. 3 to Fig. 8.

Fig. 3: Top view of mobile shoe

Fig. 4: Side view of left shoe with laser

Fig. 5: Kit Snapshot

Fig. 6: Side View Of A Mobiokle Shoe (Right Shoe)

Fig. 7: Motor and Wheels Attached

Fig. 8: Bottom View of the Right Shoe to the Mobile Shoe

Fig. 9: Mobile Shoe Attached With Hardware

IV. CONCLUSION AND FUTURE SCOPE

The proposed project, light sensing mobile shoe has a greater application in the medical field. The light sensing mobile shoe for the paralytic patients has been successfully constructed. This shoe can be utilized by the paralyzed persons to move like normal persons at cheaper cost. This shoe is implemented on many persons. The shoe works successfully. The advantage of this project is that the paralyzed person can move independently without the help of others. This project is implemented only for one leg paralyzed persons. In future it can be implemented for persons having two legs paralyzed.

REFERENCES

[1]. G. D. Fulk and E. Sazonov, "Using Sensors to Measure Activity inPeople with Stroke," submitted to Topics in Stroke Rehabilitation, 2010.

[2]. Lloyd-Jones D, Adams RJ, Brown TM, et al. Heart Disease and Stroke Statistics--2010 Update. A Report from the American Heart Association. Circulation. Dec 17 2009.

[3]. Jorgensen HS, Nakayama H, Raaschou HO, Olsen TS. Stroke.Neurologic and functional recovery the Copenhagen Stroke Study.Phys Med Rehabil Clin N Am. Nov 1999; 10(4):887-906.

[4]. E. Sazonov, G. Fulk, J. Hill , Y. Schutz and R. Browning,"Monitoring of posture allocations and activities by a shoe-basedwearable sensor", to appear in IEEE Transactions on Biomedical Engineering,2010.

A SURVEY ON GESTURE RECOGNITION TECHNIQUES IN GESTURE-BASED HUMAN COMPUTER INTERACTION INTERFACES

Sunanda Biradar[1], Ashwini M Tuppad[2]

[1,2] *Dept. of Computer Science & Engg., BLDEA's VP Dr. P G Halakatti Engg. College, (India)*

ABSTRACT

With the advent of newer techniques for the design of human computer interaction interfaces, there has been a surge in modern technologies that enable more intuitive form of communication forms. This is in contrast to the traditional console and graphical user interfaces, which restricts the process to physical device input. With availability of powerful platforms coupled with end user's demands, user interfaces are coming up with convenience incorporated within for its users. One such interface becoming more widely used nowadays is gesture based interface, where user's gestures mostly using the hands, are recognized and mapped into appropriate commands for computer operation. This paper introduces the concept of gesture recognition and reviews the literature on gesture recognition approaches, technologies utilized to implement the same to meet today's demands of human computer interaction.

Keywords: Gesture, Interface, Intuitive, Recognition, Taxonomy

I INTRODUCTION

Computers have evolved from a long history of technological advances and attempts by the designers and developers of new ways of its usage, and in proving their usefulness and ease of operation to the end users. In any field, computers need to have some sort of communication by its users and vice-versa.

The user interfaces are the means that make possible human computer interaction(HCI). Of these the traditional ones were the cumbersome console interfaces, that proved to be inconvenient for the general end users. They usually tend to have lack of computer command-specific knowledge and weren't used to the idiosyncracies inherent in command line consoles. But the developers were very well versed in it. Next, came the graphical user interfaces (GUIs) bringing revolution in computer industry by making possible Human Computer Interaction smooth and appealing to non-developer end user community due to features like icons, windows, menus and a mouse as a pointing device that could select a graphical object and navigate as per the user's choice. Again GUIs limited the scope of interaction to keyboard and mouse or such sort of physical devices. Others HCI interfaces include switch interfaces, which used buttons, audition interfaces in the form of beeps, alarms, turn by turn navigation commands when using GPS and haptic devices that generate sensations from body parts like skin [14]. The gesture-based HCI interfaces have begun to flourish and are the main research sources in this area.Interaction between any two agents, either both humans or between a human and a machine can be accomplished in two modes. First mode is verbal communication that is in terms of written or vocal

natural language sentences. The second being non-verbal communication [1], which can take the forms of sign language, gestures made by hands or other body parts, body language etc.

Hand gestures are widely used in gesture recognition systems. Again the hand gestures are categorized as static ones that involve motionless hand gestures and the dynamic category involves gestures made while hand is in motion [1]. To understand gesture based interface, the prime requirement obviously has to be understanding gestures, their interpretation, gesture enabling technologies, system response of input gestures and the application domain for which this interface is being designed [14].

II BACKGROUND

This section will throw light on the essential concepts involved in understanding different classes of gestures. In order to interpret the hand gestures by a hardware or software system, it must primarily detect the gesture based on certain features of the hand. Thus the anatomy of human hand is necessary, which will also be dealt with here.

1. Gesture Style Classification

Classification of anything becomes very easy and better if a taxonomy is presented. [14] presents a well-organized gesture style taxonomy based on the means used to make the gestures.

- Deictic gestures: Characterized by pointing using fingers, which would be a direction towards the position of an entity on a display. Their common use is to move the entity over the screen or display virtually within the problem domain.
- Gesticulation: Constitutes hand movements along with user's speech in order to interpret one's gestures. It would be more advantageous as speech and hand movements will result in more clearer understanding, but both inputs need to be synchronized.
- Manipulative gestures: Involve mapping of movements of the arm onto a location on coordinate system determined by the movements. The coordinate system refers to one that is internally used by the computer system display.
- Semaphoric gestures: Those that use hand or arm symbols that are universal across communities of people in their interpretation.
- Language gestures: Involve a set of hand gestures exclusively for one particular language, whose sequences represent distinct grammatical structures. There can be many different linguistic gesture systems for many different languages.

The interface must be designed based on application domain within which it has to work and based on suitable technologies for recognition and mapping gestures into outputs.

2. Anatomy of the human hand

Anatomy is a word from biology, which is a branch that relates to the study of the structure of a body part. As the focus of this survey is on hand gestures, structure of hand and its features must be understood thoroughly. The reason behind this is, while detection of gestures the features or signals generated by the hand guide the

process. They act as inputs to the hand gesture recognition techniques, which will ultimately be interpreted correctly and mapped onto commands for computer operation

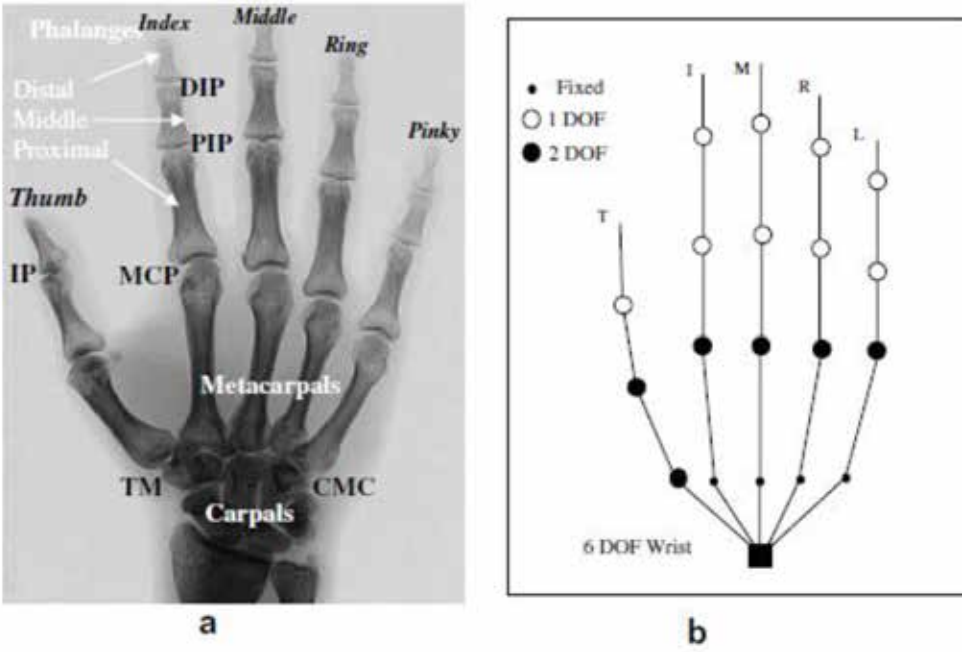

1. a: Hand gesture anatomy 1. b: Hand kinematic model.

Fig.1. structure of human hand from [2]

The skeleton of the human hand consists of 27 bones: the eight short bones of the wrist or carpus organized into a proximal, which articulates with the skeleton of the forearm, and a distal row, which articulates with the bases of themetacarpal bones (i.e. the bones of the palm or "hand proper"). The heads of these Metacarpal bones will each in turn articulate with the bases of the proximal phalanx of the phalanges. These articulations result in the formation of themetacarpophalangeal joints, which are colloquially referred to as the knuckles of a clenched fist. The fixed and mobile parts of the hand adapt to various everyday tasks by forming bony arches: longitudinal arches (the rays formed by the finger bones and their associated metacarpal bones), transverse arches (formed by the carpal bones and distal ends of the metacarpal bones), and oblique arches (between the thumb and four fingers). Of the longitudinal arches or rays of the hand, that of the thumb is the most mobile (and the least longitudinal). While the ray formed by the little finger and its associated metacarpal bone still offers some mobility, the remaining rays are firmly rigid. The phalangeal joints of the index finger, however, offer some independence to its finger, due to the arrangement of its flexor and extension tendons [14].

The hand kinematic model [2] depicts the degrees of freedom, the number of directions of movements at that point. The study of the kinematic model is important as it helps to know the kinds of motion of hand and the parameters that characterize any movement, in turn a dynamic gesture features.

II GESTURE RECOGNITION : APPROACHES AND TECHNIQUES

Gesture recognition process itself includes a number of stages, starting from hand gesture image acquisition with final stage being the mapping of recognized gesture into appropriate computer commands, which will

achieve the goal of interacting with computers using gestures. The fig.2 shows the stages involved in this process.

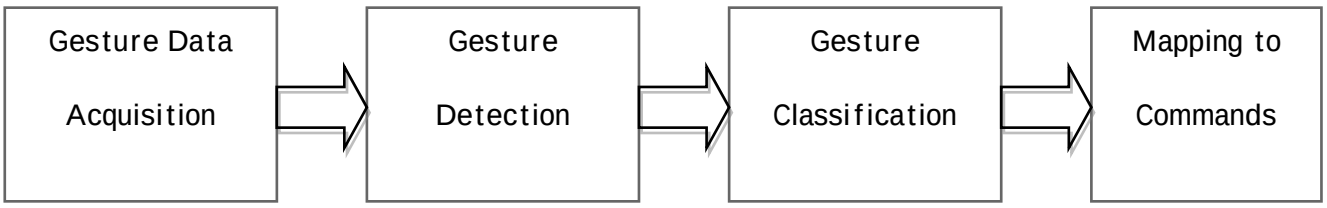

Fig.2. Gesture Recognition Process Stages

2.1 Gesture Data Acquisition

The first stage is the acquisition of data representing the gestures made by the human's hand. Gesture data acquisition accomplishment is made possible by hardware driven acquisition approach, like the sensors in the form of electrical signals or by computer vision approach where a video camera would capture an image(s) of gesture(s).

· *Hardware driven acquisition approach*

The gesture data is in the form of signals acquired by sensors held or worn on hand. Electromyogram (EMG) sensors, accelerometers, data gloves are some common means of getting signals generated by the hand while gesturing in the form of equivalent electrical signals.

Accelerometers are the electromechanical sensors that percept large, distinct gestures formed by the trajectory of forearm while it is moved [3]. Accelerometers come as analog and digital devices. The acceleration of the hand while movements is converted into a continuous voltage signal. In case of digital one, the result is a square wave, the height of whose pulse indicates the acceleration of hand [3]. But accelerometers might not sense some subtlelities, gestures with minute details involved in finger or hand movements. This can be overcome if EMG sensors are used that capture various size and scale gestures [3]. EMG sensors work by producing electrical impulses proportional to the muscular movements of the hand. Apart from these, data gloves have flex sensors embedded into it, whose resistance varies by twisting [11]. The limitation of data glove lies in the fact that they are wired and inconvenient to bear them for the duration of interaction.

· *Computer Vision Approach*

In contrast to former approach, computer vision acquisition of gesture data relies on imaging of gestures and using image analysis techniques to classify them correctly. They utilize mostly video cameras as a separate unit or web cameras mounted onto the computer as tools to acquire images. Computer vision approach can be further divided into two techniques: appearance-based and 3D model-based techniques [12]. In appearance-based technique, the gesture input image is compared with a reference hand gesture image previously stored in the computer for match of features like contours, color distribution for recognition of specific gestures [12]. The images for specific gestures are stored a priori in the database and multiple sample images for each gesture can be taken for empirical analysis. The 3D model based technique focuses on working on the degrees of freedom of

hand and its various joints while a gesture is made [12]. The analysis of image over 2- or 3- dimensions is done to infer the results by comparing with actual values of parameters and those seen in image.

2.2 Gesture Detection, Recognition

This stage involves detection of presence of gesture, not the specific gesture identification. It is done by detecting the electrical signals or image parameters that would track that the signal or image represents some or the other gesture. It is decided by looking at the pattern of magnitude, shape and other characters of signal or of the features found in the input image.

A gesture detection technique may use more of hardware components or software modules or both coupled together. It depends on the application domain, precision of recognition required, budget and system resource availability constraints, and lastly parameters like convenience, robustness etc. Generally a system that is hardware-based is costly compared to purely software like based on image processing, neural network or other concepts used as the foundation. The paper by T. Ulu et. al.[11] uses mostly hardware implementation using data gloves for gesture recognition to achieve HCI. The glove has five flex sensors to detect gesturing, embedded in it: two for index and middle fingers, with one for the thumb. They are sensitive to movement of joints in these fingers and record the bending in terms of its resistance that is proportional to bending in the fingers. In order to send the detected data to computer via microprocessor, a bridge circuit and a power amplifier circuit is used. A fast analog multiplexer to reduce 5 repetitions of the circuits for five sensors is prevented by using multiplexer that connects amplifier & bridge. An artificial neural network(ANN) is used to create a neural circuit representing the network of connections between the various bones and joints of the hand. The hidden layer of ANN has been built using 50 neurons apart from 5 neurons for input and 5 for output. The angular positions of 8 junction points detected by sensor is sent to ANN, which simulates the output hand image with sensed angular positions displayed on output part of ANN. But these circuits are prone to noisy input signals due to addition of sensor noise, impedance noise, interference noise etc. The ANN was found less sensitive to noise errors generated by sensors and tolerated use of different users[11] as experimented by the authors.

Gesture classification is extremely difficult as ambiguity between similar gestures that have to be distinctly recognized is essential. Adding to the complexity is the scientific reason that between two gesture actions, the muscular movements vary instantaneously. The magnitude of muscular motion of hand motion instantly drops to near zero when the arm relaxes after a gesture, then it increases to its actual value for second gesture [3]. Clarity in the magnitudes of hand movements gets seriously reduced. Zhang Xu et. al. [3] have presented a hand gesture recognition and virtual game control system using Electomyogram (EMG) signals and 3D Accelerometer(ACC) sensors as fusion sensor system to widen applications of it. The advantage of the process is it uses multi-channel EMG sensors thus amplifying the signals. EMG sensors are in the form of a band put on forearm of the hand, which have multiple (four) channels for signal passage to amplify the signals and provide clarity. They have used the term active segments to refer to the multi-channel signals of gestures, which represent some semantics with each such gesture. The 3D accelerometer used is a two mutually perpendicular 2D accelerometer combination, placed on the back of forearm near the wrist. Segmentation of EMG signals follows the procedure of dividing active segments into frames and representing each frame as 4n- dimensional feature vector. The average signal of the multiple EMG channel is calculated and thresholding is described for segmentation of ACC signal stream in sync with EMG signal stream. Feature extraction of the 3D ACC stream

in each active segment consists of two steps: scaling and extrapolation. Scaling of amplitude by linear min-max scaling method followed by linear extrapolation to get temporal lengths of all 3D ACC data sequences same is employed. Recognition is using Hidden Markov Model(HMM) [12], a stochastic process that takes time series of observation data as input. The output of the HMM is the probability that the input data is generated by that model. The testing is done on controlling virtual Rubik's cube game. The results of the proposed method in paper [3] for EMG+ACC were recorded the highest accuracy, nearly 100%. Results for EMG-only condition were between 65.9-80.3% and for ACC-only condition between 85.5-90.7%. The large standard deviations of the accuracies for EMG-only and ACC-only indicated that several gestures were unclassifiable. The recognition results achieved by the author's proposed system were considered satisfactory as the overall accuracy was 91.7%.

Computer vision based gesture recognition systems use image processing principles and methods. One important challenge here is the effect of background illumination over correct detection and gesture recognition. It has been addressed by devising a technique by Yoo-Joo Choi et. al. [8], the object(hand) detection phase has been done using image processing of input hand gesture image. The background image region is first separated by extracting the region based on the difference of mean and standard deviation of hue, hue-gradient of background image pixels in input image and background image. A background model of image is built for this purpose. To tightly extract the foreground image, an object bounding box is created using eigen value and vector of initially extracted image. Hand region is obtained by segmenting foreground object region into 16 sub-regions, whose histogram is produced based on number of edges in each sub-region Recognition of gestures is based on support vector machine(SVM) that is trained with sample hand shape features, multiple class for distinct hand shapes are trained followed by testing and classification. 1620 images – 180 images per hand sign for 9 different classes were captured. The mean success rate of recognition on the 9 hand signs was as seen as 92.6%.

Static gestures are focused by many researchers to establish HCI. But a dynamic user interface involves real-time gesture tracking with all the complexities previously cited. S.M. Hassan Ahmed et. al. [6] have discussed real-time, static and dynamic hand gesture recognition for Human-Computer Interaction with the aim of developing a prototype system for controlling Microsoft PowerPoint™ presentations. They have used motion detection by Fast Accelerated Segment Test(FAST) to detect the finger tips. The zest of FAST is to operate on a binary input image, traversing over the region, identifying white pixels(hand region) within a circle of radius r_{finger} drawn using Bresenham's algorithm[15] and noting the maximum number of black pixels on the circle as N_b. N_b should be greater than the maximum threshold N_{min} based on geometry of fingers. If this condition is true, then the outline separating black and white pixels would be a potential fingertip corner. Bresenham's circle algorithm exploits the circle property of being highly symmetrical, and uses it to drawing them on a display screen. It calculates the locations of the pixels in the first 45 degrees[15]. The circle is translated to a location {(x+cx), (y+cy)}, where (x,y) is current position and (cx,cy) its actual center. It then calculates pixels similarly in each of the remaining octants of the circle. Adaptive resonance theory (ART) is used for gesture classification a theory based on aspects of how the brain processes information. The ART model is that object identification and recognition generally occur as a result of the interaction of 'top-down' observer expectations with 'bottom-up' sensory information. The model postulates that 'top-down' expectations take the form of a memory template or prototype that is then compared with the actual features of an object as detected by the senses and are

recognized based on match between template and extracted object of interest. Dynamic gestures were detected using the trajectory formed by the center of the hand over a finite amount of time. Mutiple classes of gestures were given for test of which error occurred when there was little space between the fingers and ambiguity in gesture interpretation. A classification rate of 75 % was achieved for identifying the gestures used as described by the authors [6].

Routaray, S., Agarwal, A. [1] have proposed a dynamic user interface design for HCI using gestures. The image of hand acquired by a web camera is subjected to background elimination by converting each frame into two level gray scale image by removing static backgrounds. Region-based segmentation is used to extract region of interest, with object tracking using average shift calculation. Features like contours of hands are extracted, whose convex hull is obtained and recognition is comparing with predefined classes of gesture images. Recognition extracted features were classified into 11different classes, interpretation was done by mapping to particular class. Generating actions related to gesture as commands was taken as execution of the process. Recognition rate for gestures used in system were 92% for move backward gesture, followed by move forward gesture with 83.3% recognition, zoom out gesture having a rate of less than 66.8% , zoom in, rotate clockwise and rotate anticlockwise were depicted having recognition rates of 73.3%, 70% and 80% respectively on 30 users [1].

Gesture recognition involves basically complex pattern matching in terms of hand posture's static and dynamic features. Pengyu Hong et. al. [4] propose one such method based a finite state machine modelled as a sequence of states in spatial-temporal space. Each state can jump to either itself or its next state. The spatio-temporal information of a state and its neighbour states specifies the motion and the speed of the trajectory within a certain range of variance. Each state *Si* has 5 parameters : a 2D spatial centroid of a state, spatial covariance matrix, spatial threshold and a pair of minimum and maximum temporal units. The system is trained for each possible gesture that it is expected to recognize. Gesture recognition is thought as string matching between a data sequence and the state sequence of an FSM. The Knuth-Morris-Pratt (KMP) algorithm a fast string-matching algorithm, to speed up the recognition procedure. The algorithm uses a prefix function, that encapsulates the information about how a pattern matches against shifts of itself.

The experimental results for hand gestures were recognition rates with 90% or better. For mouse gestures, rates were as low as 70% for complex gestures and 90-100% for simpler gestures [4].

Virtual reality applications are potential applications of HCI through gestures. They involve moving, pointing and manipulating virtual 3D objects by the user giving a real world feel. They are also called augmented reality. Augmented reality (AR) is this technology to create a "next generation, reality-based interface"[9] and is moving from laboratories around the world into various industries and consumer markets. AR supplements the real world with virtual (computer-generated) objects that appear to coexist in the same space as the real world [10].

R.G. O'Hagan et. al [5] have presented a paper on visual gesture interface for virtual environments. The authors use a Barco Baron projection table, that provides a virtual working environment as horizontal table/vertical wall/as an inclined wall. Stereo shutter glasses are the products that are capable of creating a virtual 3D view of objects, is used to display the images of hand on the projector. A twin-camera system, mounted on projection table and right-hand coordinate system with cameras at x-axis, y-axis and the z-axis moving through the scene on display. The images are sent to the computer via the processor for image processing. A model is developed to

create templates for each of the gestures to use it as a reference to narrow down the search during feature extraction. Color-based segmentation is employed. Normalized skin color detection to track the hand is used. The pixels in skin color region are extracted. The largest connected region is detected as hand and small holes are filled. Feature extraction includes moment, high curvature detection, area, principal axes are used to obtain regions of interest like wrist, finger bases, wrist. Template matching with a confidence value indicating the amount of precision of matched feature is used for tracking. Classification of gestures is based on a statistical classifier : a logistic regression which uses a probability-based equation that takes value 0 for image features predictor parameter when it doesn't match for a certain class of gesture; it takes 1 if the image features match the class of gesture for which probability is being calculated. Positional accuracy as found out by experiment by author by measuring the location of 120 points in a plane at 100 mm intervals from 1300 to 1700 mm away from cameras [5].

III CONCLUSION

As the human society is moving towards modernization and computerized, the demand for innovation and ease of use is overly increasing. An intuitive, realistic interface for human-computer interaction is acutely needed. In this regard, the evolution of user interfaces plays an important clue in determining the way progress is seen in user interface design, driven by end user needs. The survey on all the technologies that have come so far will make us to anticipate future desires. Gesture recognition is advancing towards providing the end users a comfortable interface that would free a user from the peculiarities of the machine world. The smart technological developments in this field will bring the coming generations to contribute for making the world much easier, much appealing than ever.

REFERENCES

[1] Rautaray, S.S. and Agrawal, A., "Design of gesture recognition system for dynamic user interface", IEEE International Conference on Technology Enhanced Education, pp. 1-6, 2012.

[2] Rafiqul Z. Khan & Noor A. Ibraheem,"Gesture Algorithms based on Geometric Features Extraction and Recognition"

[3] Zhang Xu, Chen Xiang, Wang Wen-hui, Yang Ji-hai, Vuokko Lantz, Wang Kong-qiao, "Hand Gesture Recgnition and Virtual Game Control Based on 3D Accelerometer and EMG Sensors", Proceedings of the 14th international conference on Intelligent user interfaces, ACM, pp. 401-406, 2009.

[4] Hong, P., Turk, M. and Huang, T. S., " Constructing finite state machines for fast gesture recognition", Proc. ICPR '00. Los Alamitos, CA: IEEE Press, pp. 691—694, 2000.

[5] O´Hagan, R.G., Zelinsky, A. & Rougeaux, S. , " Visual Gesture Interfaces for Virtual Environments", Interacting with Computers, Vol. 14, Nr 3, pp. 231-250, 2002.

[6] S.M. Hassan Ahmed, Todd C. Alexander, and Georgios C. Anagnostopoulos, "Real-time, Static and Dynamic Hand Gesture Recognition for Human-Computer Interaction", Electrical Engineering, University of Miami, Miami, 2009.

[7] Feng-Sheng Chen, Chih-Ming Fu, Chung-Lin Huang, "Hand gesture recognition using a real-time tracking method and hidden Markov models", Image and Vision Computing 21, Elsevier, pp. 745–758, 2003.

[8] Choi, Yoo-Joo., Lee, Je-Sung, Cho. We-Duke, "A Robust Hand Recognition In Varying Illumination", Advances in Human Computer Interaction, Shane Pinder (Ed.), 2006.

[9] T. Jebara, C. Eyster, J. Weaver, T. Starner, and A. Pentland. Stochasticks, "Augmenting the billiards experience with probabilistic vision and wearable computers", In ISWC'97: Proc. Int'l Symp. On Wearable Computers, pp. 138–145, IEEE CS Press, pp.13-14, 1997.

[10] D.W.F. van Krevelen and R. Poelman. "A Survey of Augmented Reality Technologies, Applications and Limitations", The International Journal of Virtual Reality, 9(2), pp.1-20, 2010.

[11] T. Ulu, G. Cansever, IB Kucukdemiral, "An ANN Based Electronic Glove for Human-Machine Interaction", Proc. Int. Symp. on Innovations in Intelligent Systems and Applications (INISTA'05), Istanbul, Turkey, pp. 191-194, 2005.

[12] Noor A. Ibraheem & Rafiqul Z. Khan, "Vision Based Gesture Recognition Using Neural Networks Approaches: A Review", International Journal of human Computer Interaction (IJHCI)), Volume (3) : Issue (1) , 2012.

Books :

[13] Karam, Maria and Schraefel, M. C., A Taxonomy of Gestures in Human Computer Interaction, (ACM Transactions on Computer-Human Interactions, 2005).

Website links:

[14] Wikipedia website

[15] Blog link: http://www.asksatyam.com/2011/01/bresenhams-circle-algorithm_22.html

AN APPROACH TO PREVENT CASCADING FAILURES OF MULTI-CONTROLLERS IN SOFTWARE DEFINED NETWORKS

[1]Ashish Kumar Dhanotiya, [2]Saumya Hegde

[1] Scholar, [2]Assistant Professor, Department of Computer Science and Engineering,

National Institute of Technology, Surathkal, Karnataka (India)

ABSTRACT

Currently SDN designs for data centers are using multiple controllers to control the data center network and datacenter traffic. Since the traffic in the data center network is very huge, so a single controller cannot control the whole traffic, so to solve this problem some recent proposals suggested use multiple controllers. In this paper, we are focusing on the cascading failure of controllers. When a controller gets overloaded then it fails and switches under this controller will be assigned to another controller randomly, so the load of the failed controller is nonmoving to other controllers which may exceed the capacity of other controller and cause them to fail and then load of this controller also moves to other controllers and in a similar wait may cause failure of other controllers also, this will cause the cascading failure of the controllers. Here we are proposing away to prevent the controllers from cascading failures. Initially we will show a scenario for cascading failures of controller's and then propose a strategy to prevent cascading failure.

Keywords: Controller, Control Plane, Cascading Failure, Data Plane, Flow Rules, Reliability, Software Defined Networks.

I. INTRODUCTION

Present computer networks are huge and complex to control and manage, there are many equipment involved in computer networks like routers and switches, firewalls, network address translators, intrusion detection systems [1]. When a large number of end systems are added it becomes difficult to adjust the network infrastructure. SDN separate control plane from network devices. A centralized controller performs the control operations. Every time when a packet from a new flow comes to a switch, it contacts to its controller for flow rules. The Controller decides the rules to handle the packets and it gives instructions to the switches. And packets are forwarded by the switches based on the controller instructions.

Software Defined Networking gives hope to change the current network infrastructure limitations [1]. It decouples the control plane and data plane and converts the network switches to simple forwarding elements and a logically centralized controller implements the control logic. As it is clear that the whole network depends on the controller so if a controller fails SDN networks will not be able to forward the packets, so the reliability of the network is important, and it depends on the reliability of the controller. Since networks with one controller suffer from a single

point of failure so to prevent this multiple controllers are used [2]. In multiple controller approach if one controller fails then other controllers are ready to take the responsibility of switches which were under the control of that failed controller.

So the reliability of SDN network is increased by the use of multiple controllers. These multiple controllers cannot assure the reliability of the network because if one controller fails, then its load is shared by other controllers, and there is no optimal strategy in between these controllers by which we can assign the switches of failed controller to these controllers so that it will not lead any further controller failure.

Load on the controller: We are considering load as a main parameter for the failure of the controller. In SDN, for load on controller we mainly consider the number of PACKET_IN messages or the number of flow requests and installing the flow rules. Heavily loaded controllers always have higher probability of failure as they have fewer resources to handle the load [4]. Sometimes the failure of a controller may cause cascading failures of other controllers [3].

Cascading Failure: If there is a system in which there are many parts and each part is interconnected and dependent on the other parts for their reliability and survival or we can say that every part is sharing some load of the system and ready to take the extra load if any part of the system fails. If a part fails and its load is taken by another part and causes failure of that part and this process continues to the failure of other parts and thus causes the failure of the whole system, this failure is known as cascading failure. Computer networks can also suffer from cascading failures. In computer networks the traffic is forwarded by routers and switches along appropriate paths. So if a router or a node overloaded then it causes the failure of that node or router or it can also be caused when a router or a node is taken down for maintenance so in both the cases the traffic is forwarded through another node which causes that node to be overloaded and thus that node fails, in this way the cascading failure of network occurs.

II. LITERATURE SURVEY

IP networks which we are using from long time are complex and hard to manage. To achieve the required high level network policies, network operators requires configuring and managing every individual network device separately using vendor-specific commands [1]. Currently the control plane (which decides the forwarding rules) and data plane (which forwards traffic according to the forwarding rules provided by the controller). It reduces the innovation and flexibility of networking devices [1]. Software Defined networking is a new way to overcome these limitations and it help to increase the speed of innovation. It separates the control plane and data plane so that both can evolve separately. By separating both the planes, switches acts only as forwarding devices, and forwards traffic according to the instructions of controller. The entire load is carried by the controller only. SDN is now widely used in current networks like WAN and Data center networks. In recent years data centers are increasingly deployed at various places. Since data centers have high traffic [7], so it is very difficult to manage that much traffic, it becomes very complex structure, and a single controller suffers from single point of failure problem, if the controller fails then whole network collapse. For managing this complex structure and preventing the network from single point of failure, multiple controllers are used [5]. These multiple controllers are distributed in the data centers. Every controller has some portion of the switches. So when a controller fails then also network works properly, only the

switches under the failed controller get affected. These switches are then assigned to the remaining controllers. The main problem here is to place these controllers that are how many controllers are required and where these controllers should be placed [6]? If one controller fails then its load is handled by other controllers which may cause the failure of other controllers also [3]. In [3], author has proposed the problem of cascading failures of controllers in Software Defined Networking; here we are providing a solution to this problem.

III. MODEL FOR CASCADING FAILURE IN SDN:

In SDN controller is responsible for the whole network operations and switches only acts as forwarding devices which forwards data according to the instructions given by the controller, Currently for data center networks the traffic is huge, so multiple controllers are used to handle that traffic, every switch is assigned to exactly one controller. Whenever a new flow request comes to a switch, it asks to its controller to provide flow rule for that request, controller installs the flow rule along the path and then the traffic is forwarded, the time required to install the flow rule is known as flow setup time [2]. Thus the failure of a controller can cause the failure of the whole network assigned to it. In a current multi controller environment if one controller fails, then the switches under that controller are assigned to other controllers randomly, which may cause the failure of other controllerstoo, and this may lead the cascading failure of controllers, sothe whole network gets failed in this way[3].

In figure 1 cascading failure of controller is shown. [1] is showing when the network is working fine, in [2] the load on blue controller increases and it exceeds its capacity so the blue controller fails and its switches assigned to other controllers, [3] Now since switches of blue controller are assigned randomly so the load on green controller increases and exceeds to its capacity so green controller now fails, [4] Now the switches of the failed controllers are assigned to remaining red and yellow controllers and the load on red controller increases and exceeds its capacity so the red controller fails, [5] Now in similar way the last controller takes over all the switches and its load exceeds its capacity so it also fails and thus the whole network fails. As shown in figure 1, on the failure of one controller the load of that controller is distributed among other controllers. Currently we are having random assignment of switches so it is possible that all switches or most of the switches of the failed controller may be assigned to only a single controller and the load of the controller which takes the load of failed controller will increase. And it may increase in such a way that it can exceed to the capacity of the controller and causes the failure of that controller, in this way other controller may also fail, it is also possible that all the controllers fails and the whole network may collapse. It is easy to say that the probability of failure of an SDN network is high if the initial failed controller has the maximum load [3]

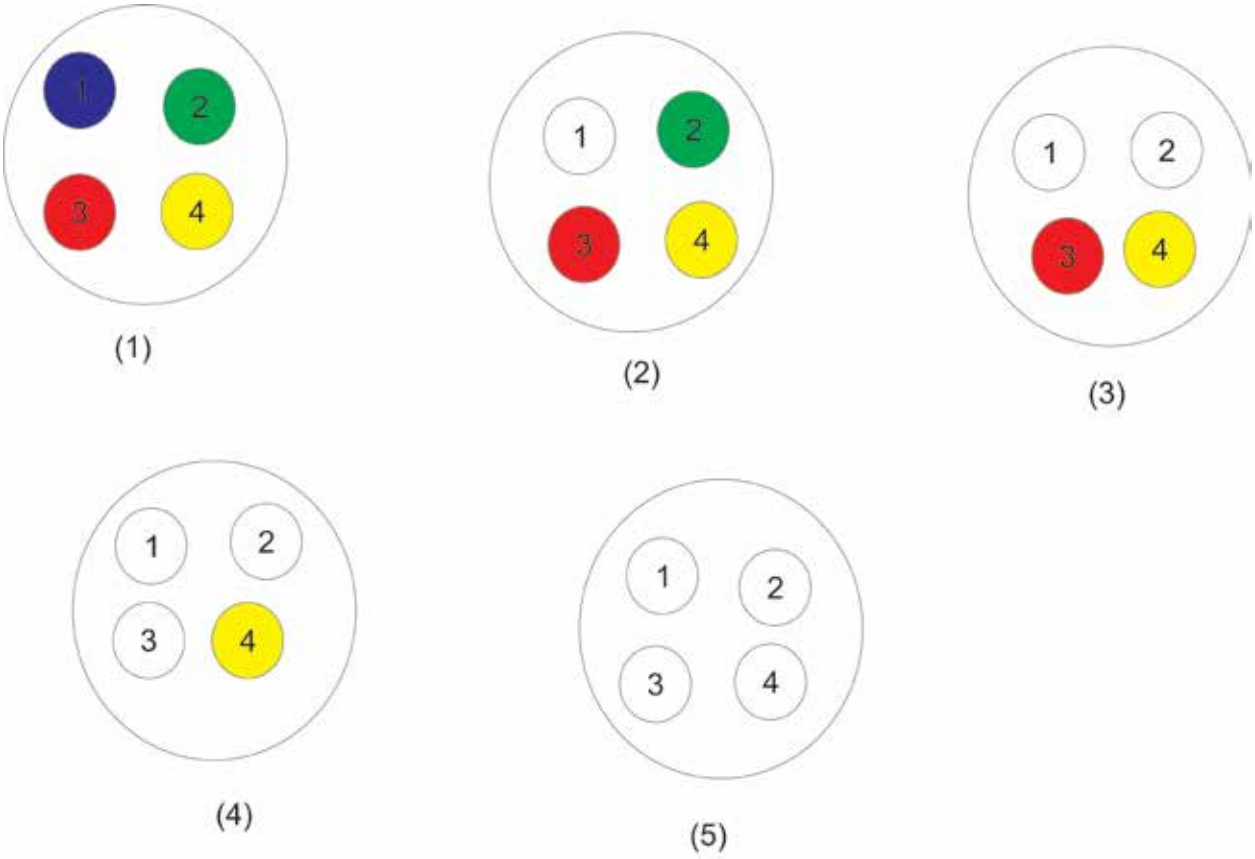

Fig.1 Cascading failure in Software Defined Networking

IV. PROPOSED SOLUTION

Currently we are not having any control over the assignment of new switches arriving at the SDN network and for the assignment of the switches of the initially failed controller. So here we are proposing a centralized controller by which we can control the assignment of switches. This centralized controller will only take care of the assignment of switches to the controllers in this way it will not have any traffic load.

In the figure2 it is shown that a single, centralized controller C is having control over all the controllers, this controller is aware of the load on each controller and their capacities. Here we are having two types of controllers' active controllers and inactive controllers. Those controllers which are having at least one switch assigned to them are known as active controllers and other controllers are known as inactive controllers. We are assuming that there are sufficient numbers of controllers to handle the whole load of the SDN network.

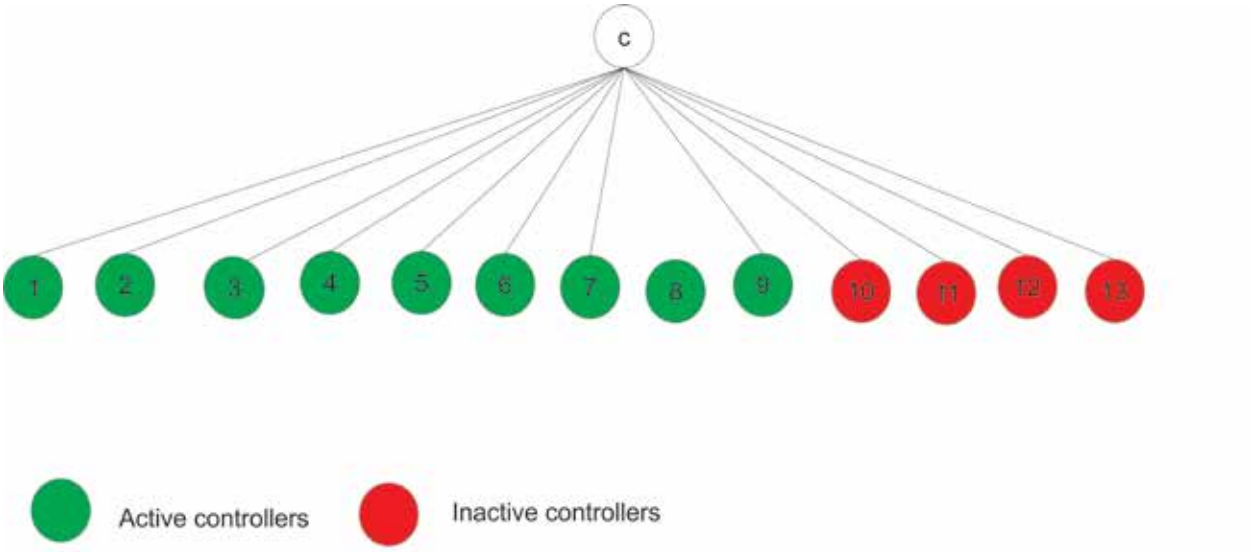

Fig.2 MultiController Environment with Single Centralized Controller

Here every time a new switch comes it requests to this central controller C for its assignment to a controller, now controller C will assign this new switch to a controller with minimum load.

And before assignment, it checks the load of the controller; if it is more than 80 percent of the capacity of the controllerthen it will not assign that switch to that controller because itmay exceed the capacity of the controller. So when centralized controllers do not find any active controller capable of handlingthe load of the failed controller it simply makes one of the inactive controllers to active and then assign switches to that controller.

When a controller in this SDN network fails then every switch under that controller will be considered as a new switch and then the centralized switch starts assignment of these switches to the controllers with minimum load and if load on each active controller exceeds more than 80 percent of its load capacity then centralized controller will make an inactive controller as an active controller and then assigns these switches to that controller, and there are not sufficient controllers then centralized controller will simply discards the requests of the switches and will not assign them to any of the controller to prevent the reliability of the controller.

V. EVALUTION

The Proposed strategy ensures the prevention of the cascading failure of the controllers as in this strategy no switch assignment is done if the load on the controller reaches near to its capacity. It is preventing the failure of initial controller, the only thing can happen is if load on a controller dynamically increases at any point of time and exceeds its capacity, then that controller can fail but it will not cause the failure of other controller. In proposed strategy, we are able to distribute load nearly in equal portions to the controllers so it will equalize and reduce the flow setup time.

This solution ensures the prevention of cascading failure of controllers by fulfilling following conditions:

1. It is ensuring that there are sufficient controllers with sufficient capacity to handle the load of the failed controller.
2. It is ensuring the balanced distribution of load among all the controllers to prevent the failure of the maximum load controller, as every controller has nearly same load.
3. The load distribution after the failure of any controller will not cause the failure of any other controller.

VI. CONCLUSION

In this paper we focused on the cascading failure problem of the controllers of the multi controller environment of data center networks when SDN is used in data center networks. Cascading failure of controllers may cause the failure of the whole data center network. Proposed strategy is well suited for preventing the cascading failure of the SDN network in data centers.

REFERENCES

Journal Papers:

[1] Diego Kreutz, Fernando M.V. Ramos, Paulo Verissimo, Christien EsteveRothberg, Siamak Azodolmolky, Steeve Uhlig *"Software-DefinedNetworking: A Comprehensive Survey," in Proceedings of the IEEE(Volume:103 , Issue: 1),2015, pp.14-76.*

[2] Md. Faizul Bari, Arup Raton Roy, Shihabur Rahman Chowdhury, QiZhang, Mohamed Faten Zhani, Reaz Ahmed, and Raouf Boutaba *"DynamicController Provisioning in Software Defined Networks," 9th CNSM and Workshops 2013 IFIP,*

[3] G. Yao, J.Bi, and L.Guo *"On the cascading failures of multi-controllersin software defined networks," in proc. IEEE ICNP, 2013, pp.1-2,*

[4] G. Yao, J.Bi, Y. Li, and L.*Guo "On the Capacitated Controller PlacementProblem in Software Defined Networks," IEEE Communications Letters,IEEE (Volume: 18, Issue: 8), pp. 1339-1342*

[5] *Kevin Phemius, Mathieu Bouet and Jeremie Leguay "DISCO: Distributedmulti-domain SDN controllers," Network Operations and ManagementSymposium (NOMS), 2014 IEEE, pp. 1-4*

[6] Brandon Heller, Rob Sherwood, Nick Mckeown *"The ControllerPlacement Problem," HotSDN'12, August 13, 2012, Helsinki, Finland.*

[7] Theophilus Benson, Ashok Anand, Aditya Akella, and Ming Zhang*"Understanding Data Center Traffic Characteristics," ACM, WREN09,August 21, 2009, Barcelona, Spain.*

DECOLORIZATION AND DETOXIFICATION OF REACTIVE RED 152 DYE BY PSEUDOMONAS SP., ISOLATED FROM TEXTILE EFFLUENT

Naresh Butani[1], Ankita Mishra[2], Ankita Anghan[3], Sunil Naik[4]

[1,4] *Naran Lala College of Professional and Applied Sciences, Navsari, Gujarat, (India)*

[2,3] *Bhagwan Mahavir College of Biotechnology, Vesu, Surat, Gujarat, (India)*

ABSTRACT

Reactive dyes are one of the most used dyes in textile industries for dyeing of cellulosic fiber. As per current trends in fashion, cotton fibers are widely utilized. Due to its chemical nature, about 40- 50% of the dyes are remaining unfixed and finally appear in the effluent. For the treatment of this effluent various chemical and physical methods are available but due its limiting factors they are not widely used. Bioremediation using bacteria is nowadays becoming an attractive alternative for the treatment of textile effluents containing dyes. In the current research work, decolorization of Reactive Red 152, a very important synthetic dye was investigated. A potential dye degrading organism, Pseudomonas sp. was isolated from textile effluent. Optimization of various physicochemical parameters like pH, temperature, various carbon source and nitrogen source were carried out for maximum dye decolorization. Under optimized condition 98% decolorization of dye is observed. The dye can be used as sole source carbon and energy source for cell growth. Phytotoxicity on wheat was tested and treated samples were found to be non-toxic. These results suggest that isolated organism Pseudomonas sp. is suitable bacterium for the bioremediation of textile waste water.

Key words: Bioremediation, Decolorization, Reactive Red 152, Reactive dye, Phytotoxicity

I. INTRODUCTION

Dyes are the coloring chemical compound having wide application in various industries like food, plastic, rubber, pharmaceutical, textile, enamel, leather, cosmetics and paper Industries[1,2]. Synthetic dyes are classified in to several group viz., direct dye, Reactive dye, disperse dye, vat dye, sulphur dyes, acid dye, basic dye etc.. Due to new fashion trends, cotton is gaining importance in the fashion industries. Reactive dyes belong to the most important group of synthetic colorants and are used extensively in the textile industries. They are used predominantly on cellulose, cellulose acetate, and acrylic fibres. Due to its low fixation on the fiber, generally 40-50% of the dyes appear in the effluent. They are generally considered as the xenobiotic compounds, which are very recalcitrant to biodegradation[3]. Unfortunately, effluent treatment facilities are not enough capable to remove the dye from the dye effluents and thus contributing toxic effects to various habitats[4]. Various alternative treatments aimed at removing Reactive dye from wastewater have been investigated, like chemical processes (Fenton oxidation and reduction)[5,6], physical precipitation and flocculation, photolysis, adsorption, electrocoagulation[7], advanced oxidation, reverse osmosis and biodegradation[8]. It is known that conventional aerobic wastewater treatment processes, such as activated

sludge, cannot efficiently remove the azo dyes. Thus, there is still a need to develop novel and effective biological decolorization processes for the cleanup of azo dyes[9]. Biological processes have gained a great attention because, due to its more cost-effectiveness and environment friendly nature than physical and chemical treatment methods, and they produce less sludge [10,11,12]. Thus, biodecolorization study of Reactive Red 152, a widely used dye is carried out. Phytotoxicity of treated and untreated samples had been studied.

II. MATERIALS AND METHODS

2.1 Chemical

Reactive Red 152 was purchased from local market of Surat textile market. Other chemicals, used in this study were of analytical grade and obtained from Hi-media, India.

2.2 Sample Collection

For sample collection various site near Surat were visited and samples were collected in sterile plastic container from Sachin GIDC, Gujarat, India. Effluent and soil samples were immediately transferred to our laboratory and stored at 4°C in refrigerator until use.

2.3 Isolation, Screening and Partial Identification of Dye Decolorizing Bacteria

10 ml of sample was mixed with 100 ml normal saline and was kept rotary shaker (100 rpm) for 1 h. After 1 h supernatant was spread on nutrient agar plate (composition : 0.5% peptone; 0.3% beef extract; 1.5 % agar; 0.5% NaCl; pH was adjusted to 7.2) and incubated at 30°C for 24 h for isolation of microorganism. Isolated organism were streaked on the BH Agar Media (Composition: TABLE 1) containing 100 ppm dye. After incubation of 72 h, potent dye decolorizing organism was selected on the basis of dye decolorization zone surrounding the colony. Isolated bacteria were maintained on nutrient agar plate. The organism was partially identified on the basis of its metabolic and morphological characteristics by BD Phoenix™.

Table: 1 Composition of Bushnell Hass (BH) Media

Component	Concentration (grams per liter)
$MgSO_4$	0.2
$CaCl_2$	0.02
KH_2PO_4	1
$(NH_4)NO_3$	1
$FeCl_3$	0.05
pH	7.4

2.4 Dye Decolorization Studies and Optimization of Physicochemical Condition

Dye decolorization experiments were carried out in 250 ml Erlenmeyer flask containing 100 ml sterile BH media containing 100 ppm dye. 5% of inoculums was transferred in the flask and kept on rotary shaker (100 rpm) at 30°C. Next day, 5 ml of sample was removed and centrifuged at 10,000 rpm for 15 min to separate biomass and supernatant. Absorbance of supernatant at λmax was recorded. Dye decolorization was measured in percent(%) dye decolorization according to following formula. An un-inoculated flask was kept as control to check the abiotic decolorization.

Decolorization (%) = A_C - A_T / A_C X 100

Where, A_C is the absorbance of the control and A_T is average absorbance of the test samples.

To ensure that the change in pH of the dye solution had no effect on the decolorization, the visible spectrum was recorded between pH 5.0 to 11.0, in which the pH did not show any effect in spectrum.

Three different carbon sources, i.e. glucose, lactose and sucrose, were tested for decolorization at various concentrations i.e. 0.2%, 0.5%, 1.0% (w/v). 2 ml of inoculum was inoculated in 100 ml BH medium along with dye and different concentration of carbon source. All flasks were incubated at 30°C on rotary shaker. Aliquot was removed for the determination of decolorizing activity at different time intervals. In the same way, two nitrogen sources were tested for decolorization of dye. The concentration of organic nitrogen (urea) and inorganic nitrogen source (ammonium chloride) were 0.2%, 0.5%, 1.0% (w/v). Effect of pH (5 to 11) and temperature (25-41°C), on dye decolorization, was also studied in the BH media containing 0.5% glucose, 0.5% ammonium chloride and dye.

2.5 Phytotoxicity Study By Seed Germination Study

To study seed germination experiment, 10 uniform sized seeds of *Phaseolus mungo* were placed in sterilized glass petridishes lined with two filter paper discs. Such three petridishes (A, B, C) were prepared. These filter discs were then moistened with 10 ml of water for control (C) and with the same volume of untreated (A) and treated (B) dye samples followed by incubation at 28°C in a BOD incubator for a period of six consecutive days to record the percent germination. The experiment was performed in triplicate[13].

III. RESULT AND DISCUSSION

3.1 Isolation, Screening and Identification of The Dye Decolorizing Bacteria

A promising dye decolorizing bacterial strain was isolated from the textile effluent sample. This strain formed a distinct clear zone on BH agar plate containing dye. To identify this bacterium, we investigated its morphological and physiological properties using various biochemical media. On the basis of results the isolate was identified as *Pseudomonas sp*. BD Phoenix is one of the reliable microbial identification system [14].

3.2 Dye Decolorization and Optimization of Physicochemical Condition

The isolated strain was tested for its capacity to remove Reactive Red 152 dye. BH media containing 100 ppm dye (as a sole source of carbon and nitrogen) was inoculated by bacterial culture. The results indicate that the strain is capable of decolorizing the dye up to 80% in 7 days. Rate of dye decolorization is presented in Fig.1. The results show that the isolated strain is effective in decolorization. Many investigators reported that reactive dyes can be used as a carbon source [15,16] and rate of the decolorization of Reactive Red 152 can be increased under optimized condition [17]. But on the other hand, some reports suggest that Reactive Red 2 could not be utilized as sole source of carbon [18]. Our results showed that Reactive Red 152 can be used as sole source of Carbon.

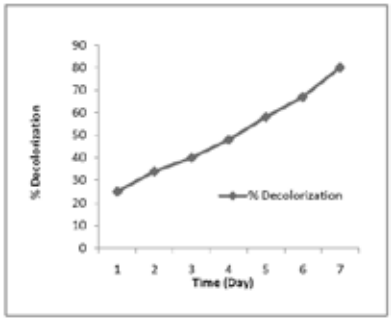

Figure 1 Decolorization of Dye

To optimize various physicochemical conditions i.e., optimization of carbon source, nitrogen source, pH and temperature, for maximum dye decolorization by isolated strains, various experiments were carried out in triplicate.. For maximum decolorization of Reactive Red 152 by the isolated strain, three different carbon sources viz., glucose, lactose and sucrose were tested. Each carbon sources were added at 0.2%, 0.5%, and 1.0% in BH medium containing 100 ppm Reactive Red 152 dye. There was increase in decolorization of Reactive Red 152 in the presence of glucose at various concentrations. Additional lactose and sucrose were not showed any significant effect on decolorization of dye.. Maximum percentage decolorization was observed when glucose was used as carbon source at 0.5% as shown in fig. 2. Two nitrogen sources urea and ammonium chloride were tested for decolorization of dyes by the isolated strain. BH medium containing Reactive Red 152 dye was supplemented with 0.2%., 0.5%, and 1.0% of urea. In the same way, experiments were carried out at 0.2%., 0.5%, and 1.0% of ammonium chloride. The best decolorization was observed when BH media was supplemented with 0.5% of ammonium chloride and 100 ppm Dye. Results are depicted in fig. 3. Effect of additional carbon and nitrogen sources were studied by many authors[19]. Our results were also supported by some author [20,21]. Our results were supported by some researcher that degradation of Reactive Red BS is increased in the presence of the glucose, peptone and yeast extract [22]. Additional nitrogen source yeast extract also showed increase in decolorization by halophilic *Pseudomonas spp.* RA20 [23].

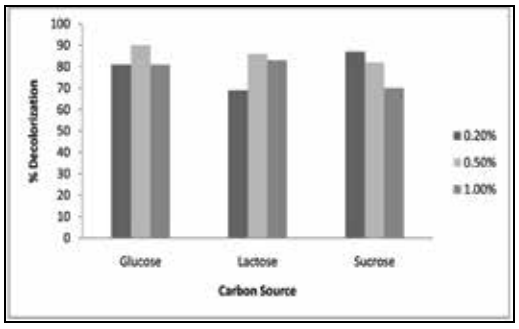

Figure 2 Effect of Carbon source on on decolorization of Dye

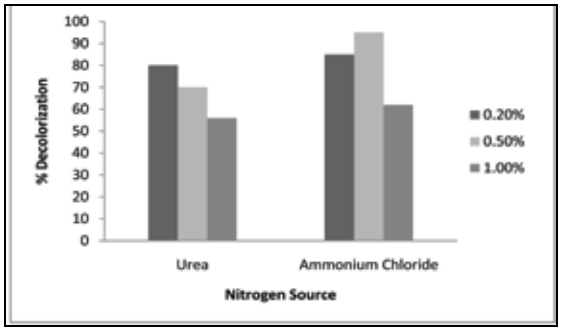

Figure 3 Effect of Nitrogen source decolorization of Dye

The effect of temperature and pH on the dye decolorization was tested. It was found that a temperature of 31°C was optimum for maximum decolorization (Fig. 4). Decline in decolorization activity at higher temperature more than 39°C can be attributed to the loss of cell viability. Optimum pH for maximum dye decolorization was 7.0 (Fig. 5). Results of some researcher support our results that Reactive Navy Blue HE2R degraded best at temp 30°C and pH 7[24].

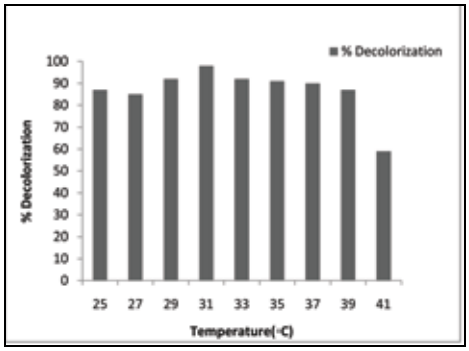

Figure 4 Effect o Temperature On Decolorization of Dye

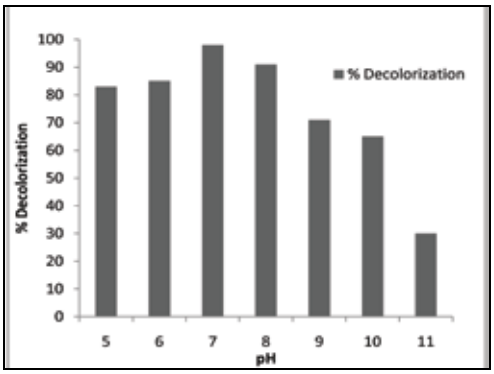

Figure 5 Effect of Ph On Decolorization of Dye

3.3 Phytotoxicity Study

Study of phytotoxicity of treated sample provides the information about the toxic nature of metabolites [25].Untreated samples exhibited 30% germination at a same time control and treated samples 100% germination.

IV. CONCLUSION

The present study has resulted in the isolation of a bacterial strain that has capacity of decolorizing Reactive Red 152, thus show the potential to be exploited as possible candidate for bioremediation. Decolorization activity can be enhanced by addition of glucose. The isolated strain can decolorize dyes under wide range of pH and temperature, which is the nature of effluent from dyeing industries.

REFERENCES

[1] K. Selvam, K. Swaminathan, and K.-S. Chae, Microbial decolorization of azo dyes and dye industry effluent by *Fomes lividus*, *World Journal of Microbiology and Biotechnology*, *19(6)*, 2003, 591-593.

[2] G.F. Liu, J.T. Zhou, J. Wang, Z.Y. Song, and Y.Y. Qv, Bacterial decolorization of azo dyes by *Rhodopseudomonas palustris*, *World Journal of Microbiology and Biotechnology*, *22(10)*, 2006, 1069-1074.

[3] I. Arslan-Alaton, and S. Dogruel, Photodegradation of hydrophobic disperse dyes and dye-bath effluents by silicadodecatungstate nanoparticles, *Water Sci Technol*, *49(4)*, 2004, 171-176.

[4] G. Annadurai, S.R. Babu, G. Nagarajan, and K. Ragu, Use of Box–Behnken design of experiments in the production of manganese peroxidase by *Phanerochaete chrysosporium* (MTCC 767) and decolorization of crystal violet, *Bioprocess Engineering*, *23(6)*, 2000, 715-719.

[5] C.L. Hsueh, Y.H. Huang, C.C. Wang, and C.Y. Chen, Degradation of azo dyes using low iron concentration of Fenton and Fenton-like system, *Chemosphere*, *58(10)*, 2005, 1409-1414.

[6] A. Aguiar, and A. Ferraz, Fe(3+)- and Cu(2+)-reduction by phenol derivatives associated with Azure B degradation in Fenton-like reactions, *Chemosphere*, *66(5)*, 2007, 947-954.

[7] N. Daneshvar, A.R. Khataee, A.R. Amani Ghadim, and M.H. Rasoulifard, Decolorization of C.I. Acid Yellow 23 solution by electrocoagulation process: investigation of operational parameters and evaluation of specific electrical energy consumption (SEEC), *J Hazard Mater*, *148(3)*, 2007, 566-572.

[8] W. Azmi, R.K. Sani, and U.C. Banerjee, Biodegradation of triphenylmethane dyes, *Enzyme and Microbial Technology*, *22(3)*, 1998, 185-191.

[9] J.K. Glenn, and M.H. Gold, Decolorization of several polymeric dyes by the lignin-degrading basidiomycete Phanerochaete chrysosporium, *Applied and Environmental Microbiology*, *45(6)*, 1983, 1741-1747.

[10] J.A. Bumpus, and B.J. Brock, Biodegradation of crystal violet by the white rot fungus *Phanerochaete chrysosporium*, *Applied and Environmental Microbiology*, *54(5)*, 1988, 1143-1150.

[11] J. Wu, L. Li, H. Du, L. Jiang, Q. Zhang, Z. Wei, X. Wang, L. Xiao, and L. Yang, Biodegradation of leuco derivatives of triphenylmethane dyes by *Sphingomonas sp*. CM9, *Biodegradation*, *22(5)*, 2011, 897-904.

[12] C.C. Chen, H.J. Liao, C.Y. Cheng, C.Y. Yen, and Y.C. Chung, Biodegradation of crystal violet by *Pseudomonas putida*, *Biotechnology letters*, *29(3)*, 2007, 391-396.

[13] R. Chandra, R.N. Bharagava, K. Atya, and H.J. Purohit, Bacterial diversity, organic pollutants and their metabolites in two aeration lagoons of common effluent treatment plant (CETP) during the degradation and detoxification of tannery wastewater, *Bioresource Technology 102*, 2011, 2333-2341.

[14] J. Snyder, G. Munier, and C. Johnson, Direct Comparison of the BD Phoenix System with the MicroScan WalkAway System for Identification and Antimicrobial Susceptibility Testing of *Enterobacteriaceae* and Nonfermentative Gram-Negative Organisms, *Journal of Clinical Microbiology*, *46(7)*, 2008, 2327–2333.

[15] A. Boonyakamol, T. Imai, P. Chairattanamanokorn, T. Higuchi, M. Sekine, and M. Ukita, Reactive Blue 4 decolorization under mesophilic and thermophilic anaerobic treatments, *Appl Biochem Biotechnol*, *152(3)*, 2009, 405-417.

[16] R.Y. Watanapokasin, A. Boonyakamol, S. Sukseree, A. Krajarng, T. Sophonnithiprasert, S. Kanso, and T. Imai, Hydrogen production and anaerobic decolorization of wastewater containing Reactive Blue 4 by a bacterial consortium of *Salmonella subterranea* and *Paenibacillus polymyxa*, *Biodegradation*, *20(3)*, 2009, 411-418.

[17] K. Kodam, and K. Gawai, Decolorisation of reactive red 11 and 152 azo dyes under aerobic conditions, *Indian journal of biotechnology*, *5(3)*, 2006, 422-424.

[18] M.I. Beydilli, and S.G. Pavlostathis, Decolorization kinetics of the azo dye Reactive Red 2 under methanogenic conditions: effect of long-term culture acclimation, *Biodegradation*, *16(2)*, 2005, 135-146.

[19] R. Olaganathan, and J. Patterson, Decolorization of anthraquinone Vat Blue 4 by the free cells of an autochthonous bacterium, *Bacillus subtilis*, *Water Sci Technol*, *60(12)*, 2009, 3225-3232.

[20] C.C. Oturkar, H.N. Nemade, P.M. Mulik, M.S. Patole, R.R. Hawaldar, and K.R. Gawai, Mechanistic investigation of decolorization and degradation of reactive red 120 by *Bacillus lentus* BI377, *Bioresour Technol*, *102(2)*, 2011, 758-764.

[21] G. Parshetti, S. Kalme, G. Saratale, and S. Govindwar, Biodegradation of malachite green by *Kocuria rosea* MTCC 1532, *Acta Chimica Slovenica*, *53(4)*, 2006, 492.

[22] N. Sheth, and S. Dave, Optimisation for enhanced decolourization and degradation of Reactive Red BS CI 111 by *Pseudomonas aeruginosa* NGKCTS, *Biodegradation*, *20(6)*, 2009, 827-836.

[23] S. Hussain, Z. Maqbool, S. Ali, T. Yasmeen, M. Imran, F. Mahmood, and F. Abbas, Biodecolorization of reactive black-5 by a metal and salt tolerant bacterial strain *Pseudomonas sp*. RA20 isolated from Paharang drain effluents in Pakistan, *Ecotoxicology and environmental safety*, *98*, 2013, 331-338.

[24] R. Dhanve, U. Shedbalkar, and J. Jadhav, Biodegradation of diazo reactive dye Navy Blue HE2R (Reactive Blue 172) by an isolated *Exiguobacterium sp*. RD3, *Biotechnology and Bioprocess Engineering*, *13(1)*, 2008, 53-60.

[25] R. Saratale, G. Saratale, J.-S. Chang, and S. Govindwar, Ecofriendly degradation of sulfonated diazo dye CI Reactive Green 19A using *Micrococcus glutamicus* NCIM-2168, *Bioresource technology*, *100(17)*, 2009, 3897-3905.

MICROBIAL DEGRADATION OF PHENOL

Tushal Mangukiya[1], Naresh Butani[2], Jaydip Jobanputra[3], Sagar Desai[4]

[1,3,4]Bhagwan Mahavir College of Biotechnology, Vesu, Surat, Gujarat, (India)

[2]Naran Lala College of Professional and Applied Sciences, Navsari, Gujarat, (India)

ABSTRACT

Effluent from chemical industries contains many organic toxic pollutants which can be hazardous to aquatic life as well as human health. Phenol is one of the most hazardous pollutants present in industrial effluents. Even at very low concentration phenol is of considerable health concern. The increasing toxicity of phenol has become warning alarm for its removal. There are many conventional method such as chemical and physical for the treatment of phenol wastes from environment. Biological treatment using microorganism has proved to be most effective and successful process for the treatment of phenolic wastes. In order to find out phenol degrading bacteria, some soil samples were collected from industrial polluted sites. After proper enrichment of the samples, microorganisms were isolated on the solid media containing phenol. Isolated microorganisms were screened on the basis of their phenol removal capacity in the liquid broth. This process was carried out in shake flask batch culture at 120 rpm for 24 hrs at 30°C using a specific concentration of phenol in ppm. Removal of phenol was estimated using 4-Aminoantipyrine method.

***Key words*: 4- Amino Antipyrine, Biodegradation, Phenol**

I. INTRODUCTION

In last few decades, humans have faced many serious environmental pollution problems, increasing tremendously every day[1]. All the types of environmental pollutions are hazardous, among which water pollution is more dangerous and is the major concern today. Many types of pollutants like organic, inorganic, suspended solids and radioactive materials are majorly responsible for water pollution[2].

Wastewater from industrial effluent contains many pollutants like phenol, which are frequently disposed without any treatment. Phenol is highly toxic, corrosive and mutagenic; it is also teratogenic agent affecting both environment and living organisms[3]. Phenol is a hazardous for humans, plants and animals, when present in low concentration. High and acute concentration of phenol can cause a central nervous system disorders and myocardial depression. It also causes irritation of eyes, swelling, corneal whitening and also blindness. When present in low concentration, it can be toxic for some aquatic species. It cause taste and odor problems in water and this water cause serious skin damage, cardiovascular diseases, gastrointestinal damage and also death[4].It is most commonly used in perfumes, lubricating oils, dyes and in the manufacture of industrial and agricultural product[5]. It enters into the natural water bodies through the effluent of many industries like high temperature coal conversation, petroleum refining, resin and plastic manufacturing, wood and dye industries. It is also found in the contaminated drinking water[6].

Due to such toxic and life threatening effects of phenol on living organisms, it is essential to remove or degrade it completely from the ecosystem[7]. Currently many different physical, chemical and biological methods are used for the removal of phenol[8,9]. Current chemical procedures for phenol removal involve many expensive methods like distillation, liquid-liquid extraction with the use of different solvents, adsorption, and membrane

pervaporation and membrane solvent extraction. However, such treatments are very complex and expensive which triggers the development of new technologies and methods for phenol removal. Biological treatments have shown to be economically viable, practical and the most promising one[10].

Despite of being toxic, phenol can be effectively utilized by microbes as carbon and energy sources. A number of studies on phenol biodegradation with the help of microorganisms have been carried out in past years. Both fungi and bacteria are known for the degradation of phenol and its derivatives whereas only a few members of yeast genera are capable of phenol degradation[11]. The aim of the present study was to isolate and characterize indigenous microorganisms, capable of degrading phenol, form industrial effluents and to establish optimal physiological parameters for phenol degradation.

II. MATERIALS AND METHOD

2.1 Sample Collection and Enrichment:

Soil and effluent samples were collected from industrial chemically contaminated sites surrounding Surat City, Gujarat, India. Samples were collected in sterile plastic container and immediately transferred to the laboratory and stored in refrigerator (4°C) till use.

Enrichment of the samples was carried out at laboratory condition by inoculating samples in nutrient broth medium with addition of 50 ppm of phenol. The flasks were kept on rotator shaker at 100 rpm. 10 ml of enriched samples were transferred in 100 ml fresh medium containing phenol. Such five successive transfers were carried out.

2.2 Isolation and Partial Characterization of Phenol Degrading Microorganism

From the enriched samples, a loop full of suspension was streaked on nutrient agar plate containing 100 ppm phenol. The plates were incubated at 37°C for 24-48 hr. After incubation the plates were observed for phenol degrading microorganisms. Partial characterization of the isolated organism was carried out by studying the morphological, cultural and biochemical characteristics.

2.3 Phenol Degradation Experiments

The isolated organism was subjected to study phenol degradation in 250 ml Erlenmeyer flasks containing 100 ml of Bushnell Hass medium containing 100 ppm phenol and 1% glucose as additional carbon source. The flasks were incubated on rotary shaker at 120 rpm. Samples were removed at regular interval aseptically and were phenol content was measured spectrophotometrically using 4-aminoantipyrene method (mentioned below).

2.4 Phenol Estimation Assay (4-Aminoantipyrine Method) [12]

Removed sample was taken in micro-centrifuge tube and centrifuge at 10,000 rpm for 20 min to remove biomass.1 ml of supernatant was added to 9 ml of Distilled water. To this mixture 0.5 ml 2N NH_4OH solution, 0.25 ml of 2% 4-aminoantipyrine solution and 0.25 ml 8% K_3FeCN_6 is added. Absorbance of red color is measured in spectrophotometer at 510 nm and compared with standard phenol solution curve.

2.5 Optimization of Various Physicochemical Parameters

2.5.1 Optimization of Ph: Effect of initial pH of the media on degradation of phenol was checked. Here, initial

pH of the BH media was adjusted to 5, 6, 7, 8, 9, 10 and 11. Inoculum (1.5 ml) was inoculated in 100 ml BH medium containing phenol. At regular interval samples were removed and checked for phenol degradation.

2.5.2 Optimization of Temperature: Effect of incubation temperature on degradation of phenol was studied. 1.5 ml of inoculums was inoculated in 100 ml BH medium containing phenol. Inoculated BH media was incubated at various temperature i.e. 25ºC, 27ºC, 29ºC, 31ºC, 33ºC, 35ºC, 37ºC, 39ºC, 41ºC.

2.5.3 Optimization of Additional Carbon Source and Nitrogen Sources: Three additional carbon sources i.e. glucose, lactose, sucrose and two additional nitrogen sources i.e. organic nitrogen source(urea), inorganic nitrogen source(ammonium chloride) were tested for the degradation of phenol at various concentration i.e. 0.2, 0.5 and 1.0%(w/v). 1.5 ml of inoculums was inoculated in 100 ml BH medium containing phenol and different concentration of additional carbon and nitrogen source. All flasks were incubated at 37ºC on shaker. Sample was removed for the estimation of degraded phenol at different time interval.

III. RESULTS AND DISCUSSION

3.1 Sample Collection and Enrichment

Seven different effluent and soil sediment samples were collected from three different chemically contaminated sites, namely Bamroli Khadi, Pandesara GIDC, and Sachin GIDC, Surat. Enrichment was done in nutrient broth media supplemented with 50 ppm phenol. The essence of enrichment technique is to provide growth conditions that are very favorable for the organism of interest, and unfavorable for competing organisms, and also increase relative population size [13,14].

3.2 Isolation and Partial Characterization of Phenol Degrading Microorganism

Phenol degrading organism was isolated, on the bases of its growth on the media containing phenol. As a result of enrichment technique, a typical colony of cream color was isolated. On the basis of morphological characteristics it may be tentatively identified as yeast. Based on cultural and biochemical conditions, the isolated organism was identified as *Candida Spp.*(Data not shown) [15].

3.3 Phenol Degradation Experiments

The isolated microorganism was tested for its potential to degrade phenol. The assay was carried out in BH medium supplemented with 100 ppm phenol. The phenol removal efficiency was observed 60% in 96 h (Fig.-1).

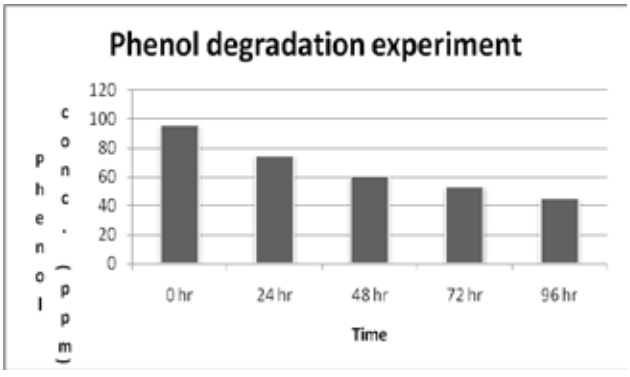

Fig.-1: Phenol Biodegradation Experiment.

3.4 Optimization of Physiological Parameters

Optimization of pH was done by adjusting the initial pH of media, result suggested that in maximum phenol degradation was observed at pH 7 (Fig.-2). Aysha OS [16] and Mumtaj K (2014) and Awan et al., (2013) [17] reported similar kind of results showing maximum phenol degradation at pH 7. Our results were supported by the work of Alexander and Robertson. They experimented that the majority of organisms could not survive in pH range below from 5.0 or above from 9.0. At high or low pH values acid or base could affect the enzyme activity of the cell [18].

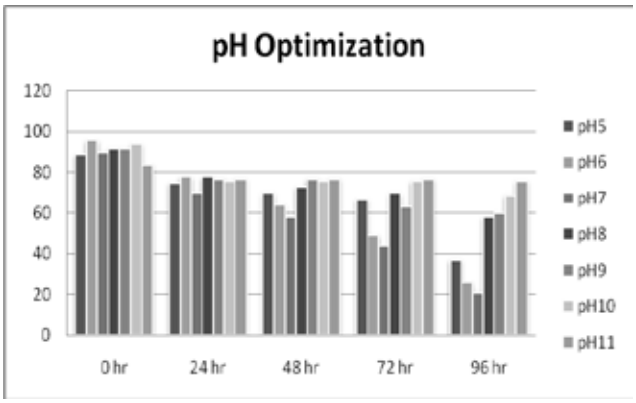

Fig.-2: ₚh OPTIMIZATION FOR PHENOL BIODEGRADATION.

Each life form has a minimum, optimum and maximum temperature for growth. For temperature optimization flasks were incubated at different temperature. These resulted in the maximum phenol degradation at 31 ºC temperature (Fig.-3). Chakraborty et al., (2010) also reported the same results for optimization of temperature for phenol degradation [19].

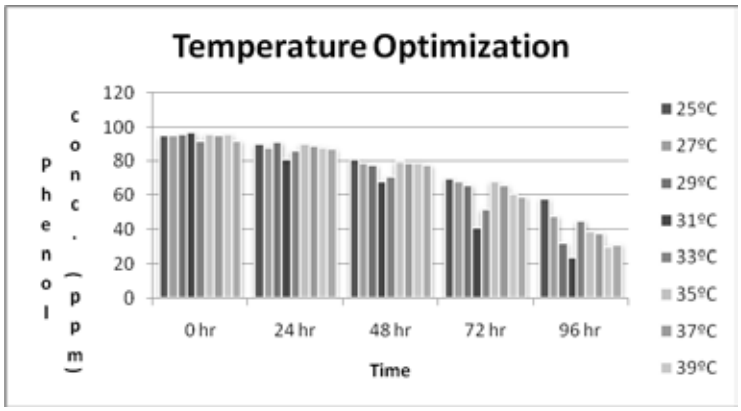

Fig.-3: Temperature Optimization for Phenol Biodegradation.

Three different carbon sources glucose, lactose and sucrose were used at the concentration of 0.2%, 0.5% and 1.0% for the optimization of additional carbon source. The maximum phenol degradation was observed in flask containing 1% glucose (Fig.-4) whereas there was no increase in the rate of phenol degradation when lactose (Fig.-5) and sucrose (Fig.-6) were added. In the previous study by the author, it was observed that 0.5% glucose was optimum for maximum biodegradation of Phenol by *Staphylococcus aureus* [20].

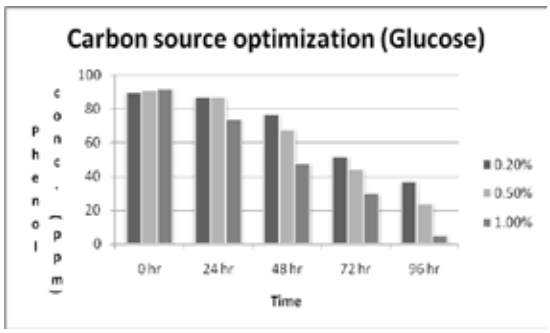

Fig.-4: Carbon source (Glucose) optimization for phenol biodegradation.

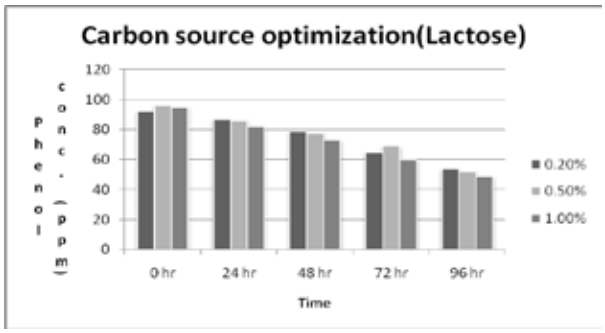

Fig.-5: Carbon source (Lactose) optimization for phenol biodegradation.

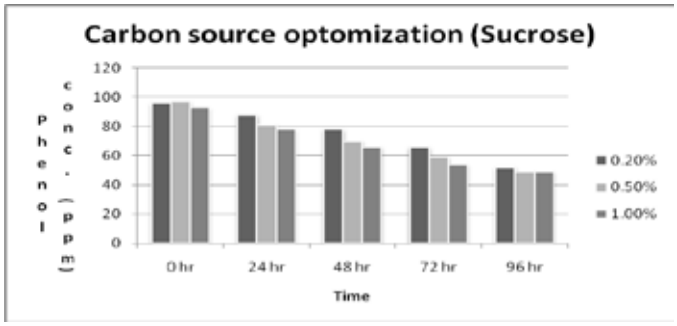

Fig.-6: Carbon Source (Sucrose) Optimization for Phenol Biodegradation.

Two different nitrogen sources (urea and ammonium chloride) were tested for the maximum phenol degradation by the isolated organism. The maximum phenol removal was observed at 1.0 % of urea (Fig.-7) and 1.0% of ammonium chloride (Fig.-8). The result suggest that ammonium chloride has impact on degradation of Phenol [20].

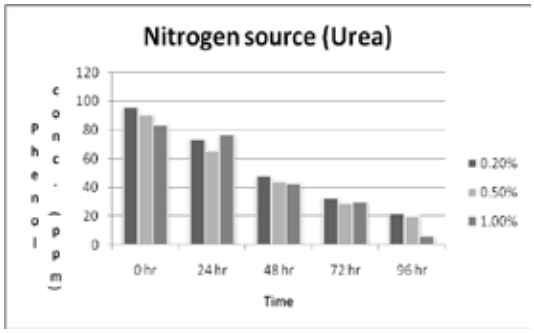

Fig.-7: Nitrogen Source (Urea) Optimization For Phenol Biodegradation.

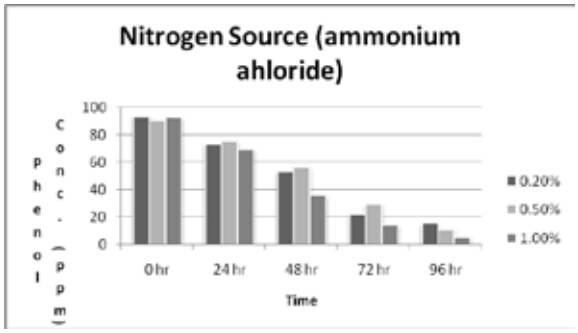

Fig.-8: Nitrogen Source (Ammonium Chloride) Optimization For Phenol Biodegradation.

IV. CONCLUSION

From this research report it can be concluded, isolated *Candida Spp*. had potential to degrade phenol. Results of optimization suggest that it can survive under harsh condition of effluent. It can be exploited as a potential degrader of phenol present in industrial effluent. Isolated strain can be used in bioremediation treatment of the industrial effluent.

REFERENCES

[1] F. Huma, M. Jaffar, and K. Masud, A modified potentiometric method for the estimation of phenol in aqueous systems, *Turkish Journal of Chemistry*, *23(4)*, 1999, 415-422.

[2] S.S. Dara, *Textbook of Environmental Chemistry and Pollution Control*, (S. Chand & Company Ltd., New Delhi, 1995).

[3] M. Kopytko, and L.A. Jacome, Alternative for phenol biodegradation in oil contaminated wastewaters using an adapted bacterial biofilm layer *Rudarsko-geolosko-naftni zbornik*, *20(1)*, 2008, 71-82.

[4] P. Kumaran, and Y. Paruchuri, Kinetics of phenol biotransformation, *Water Research*, *31(1)*, 1997, 11-22.

[5] G. Gurujeyalakshmi, and P. Oriel, Isolation of phenol-degrading *Bacillus stearothermophilus* and partial characterization of the phenol hydroxylase, *Applied and environmental microbiology*, *55(2)*, 1989, 500-502.

[6] C.I. Nair, K. Jayachandran, and S. Shashidhar, Biodegradation of phenol, *African journal of biotechnology*, *7(25)*, 2008.

[7] J. Mamatha, A. Vedamurthy, and S. Shruthi, Degradation of phenol by turnip root enzyme extract, *Journal of Microbiology and Biotechnology Research*, *2(3)*, 2012, 426-430.

[8] G. Busca, S. Berardinelli, C. Resini, and L. Arrighi, Technologies for the removal of phenol from fluid streams: a short review of recent developments, *Journal of Hazardous Materials*, *160(2)*, 2008, 265-288.

[9] M. Ahmaruzzaman, Adsorption of phenolic compounds on low-cost adsorbents: a review, *Advances in Colloid and Interface Science*, *143(1)*, 2008, 48-67.

[10] D. Tambekar, P. Bhorse, and P. Gadakh, Biodegradation of phenol by native micoorganism isolated from Lonar lake in Maharashtra State (India), *International Journal of Life sciences and Pharama Research*, *2(4)*, 2012.

[11] M. Piakong, A. Noor, and M. Madihah, Degradation pathway of Phenol through ortho cleavage by C*andida tropicalis*, *Borneo Sciences 24*, 2009, 1-8.

[12] R. Martin, Rapid colorimetric estimation of phenol, *Analytical Chemistry*, *21(11)*, 1949, 1419-1420.

[13] R. Rathnayaka, Effect of sample pre-enrichment and characters of food samples on the examination for the Salmonella by plate count method and fluorescent in situ hybridization technique, *American Journal of Food Technology*, *6(9)*, 2011, 851-856.

[14] K. Egli, U. Fanger, P.J. Alvarez, H. Siegrist, J.R. Van Der Meer, and A.J. Zehnder, Enrichment and characterization of an anammox bacterium from a rotating biological contactor treating ammonium-rich leachate, *Archives of Microbiology*, *175(3)*, 2001, 198-207.

[15] A. Novak, C. Vágvölgyi, and M. Pesti, Characterization of Candida albicans colony-morphology mutants and their hybrids, *Folia microbiologica*, *48(2)*, 2003, 203-209.

[16] O. Aysha, and K. Mumtaj, Degradation of phenol by selected strain of *Bacillus spp*. isolated from marine water, *American Journal of Pharmacy and Health Care*, *2(6)*, 2014, 41-56.

[17] Z.U.R. Awan, A. Shah, and M. Amjad, Microbial degradation of phenol by locally isolated soil bacteria, *Global Adv Res J Microbiol*, *2(4)*, 2013, 072-079.

[18] B. Robertson, and M. Alexander, Influence of calcium, iron, and pH on phosphate availability for microbial mineralization of organic chemicals, *Applied and environmental microbiology*, *58(1)*, 1992, 38-41.

[19] S. Chakraborty, T. Bhattacharya, T. Patel, and K. Tiwari, Biodegradation of phenol by native microorganisms isolated from coke processing wastewater, *Journal of Environmental Biology*, *31(3)*, 2010, 293.

[20] B. Naresh, P. Honey, and S. Vaishali, Biodegradation of phenol by a bacterial strain isolated from a phenol contaminated site in India, *Res J Environmental Sci*, *1(1)*, 2012, 46-49.